Parton Distribution Functions at the LHC

Robert Thorne

February 15th, 2013

University College London

IPPP Research Associate

With contributions from Alan Martin, James Stirling, Graeme Watt

and Arnold Mathijssen and Ben Watt

Strong force makes it difficult to perform analytic calculations of scattering processes involving hadronic particles.

The weakening of $\alpha_S(\mu^2)$ at higher scales $\rightarrow$ the **Factorization Theorem**.

Hadron scattering with an electron factorizes.

Q^2 – Scale of scattering

$x = \frac{Q^2}{2m\nu}$ – Momentum fraction of Parton (ν=energy transfer)

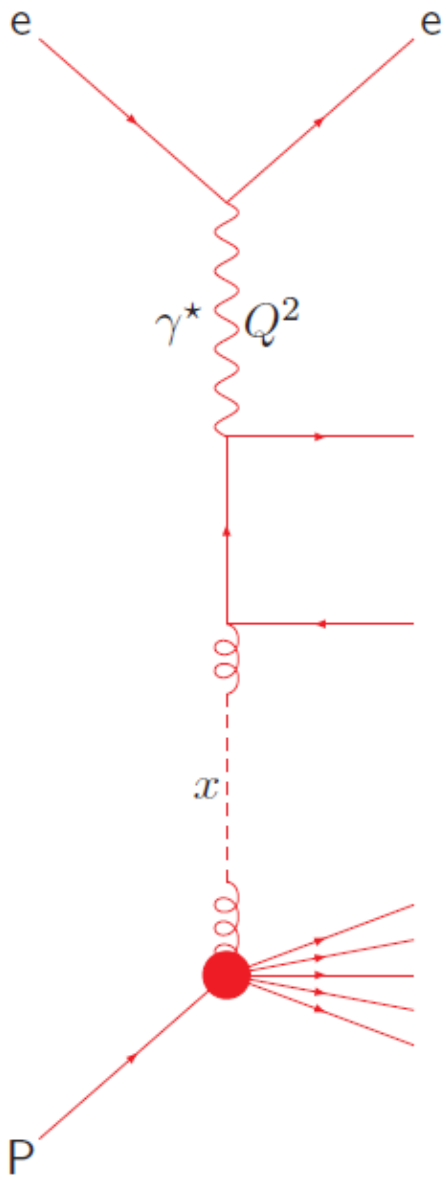

perturbative
calculable
coefficient function
$C_i^P(x, \alpha_s(Q^2))$

nonperturbative
incalculable
parton distribution
$f_i(x, Q^2, \alpha_s(Q^2))$

The coefficient functions $C_i^P(x, \alpha_s(Q^2))$ are process dependent (new physics) but are calculable as a power-series in $\alpha_s(Q^2)$.

$$C_i^P(x, \alpha_s(Q^2)) = \sum_k C_i^{P,k}(x) \alpha_s^k(Q^2).$$

Since the parton distributions $f_i(x, Q^2, \alpha_s(Q^2))$ are process-independent, i.e. **universal**, and evolution with scale is calculable, once they have been measured at one experiment, one can predict many other scattering processes.

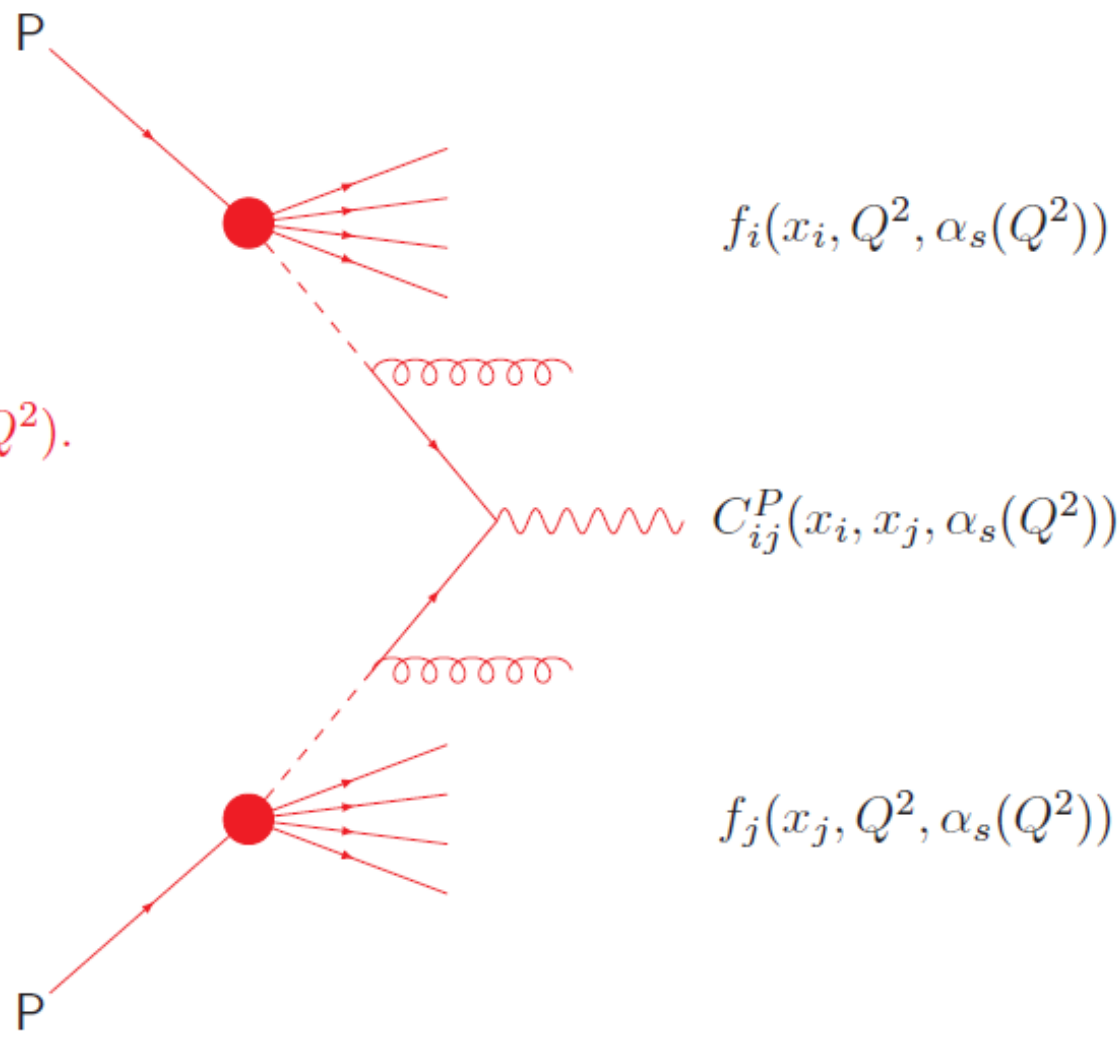

Obtaining PDF sets – General procedure.

Start parton evolution at low scale $Q_0^2 \sim 1\mathrm{GeV}^2$. In principle 11 different partons to consider.

$$u, \bar{u}, \quad d, \bar{d}, \quad s, \bar{s}, \quad c, \bar{c}, \quad b, \bar{b}, \quad g$$

$m_c, m_b \gg \Lambda_{\mathrm{QCD}}$ so heavy parton distributions determined perturbatively. Leaves 7 independent combinations, or 6 if we assume $s = \bar{s}$ (just started not to).

$$u_V = u - \bar{u}, \quad d_V = d - \bar{d}, \quad \mathrm{sea} = 2 * (\bar{u} + \bar{d} + \bar{s}), \quad s + \bar{s} \quad \bar{d} - \bar{u}, \quad g.$$

Input partons parameterised as, e.g. MSTW,

$$xf(x, Q_0^2) = (1 - x)^{\eta}(1 + \epsilon x^{0.5} + \gamma x)x^{\delta}.$$

Evolve partons upwards using LO, NLO (or increasingly NNLO) DGLAP equations.

$$\frac{df_i(x,Q^2,\alpha_s(Q^2))}{d \ln Q^2} = \sum_j P_{ij}(x, \alpha_s(Q^2)) \otimes f_j(x, Q^2, \alpha_s(Q^2))$$

Fit data above $\sim 2\mathrm{GeV}^2$. Need many types for full determination.

- Lepton-proton collider HERA – (DIS) $\rightarrow$ small-x quarks (best below $x \sim 0.05$). Also gluons from evolution (same x), and now $F_L(x, Q^2)$. Also, jets $\rightarrow$ moderate-x gluon.Charged current data some limited info on flavour separation. Heavy flavour structure functions – gluon and charm, bottom distributions and masses.

- Fixed target DIS – higher x – leptons (BCDMS, NMC, ...) $\rightarrow$ up quark (proton) or down quark (deuterium) and neutrinos (CHORUS, NuTeV, CCFR) $\rightarrow$ valence or singlet combinations.

- Di-muon production in neutrino DIS – strange quarks and neutrino-antineutrino comparison $\rightarrow$ asymmetry . Only for $x > 0.01$.

- Drell-Yan production of dileptons – quark-antiquark annihilation (E605, E866) – high-x sea quarks. Deuterium target – $\bar{u}/\bar{d}$ asymmetry.

- High-p_T jets at colliders (Tevatron) – high-x gluon distribution – $x > 0.01$.

- W and Z production at colliders (Tevatron/LHC) – different quark contributions to DIS.

This procedure is generally successful and is part of a large-scale, ongoing project. Results in partons of the form shown.

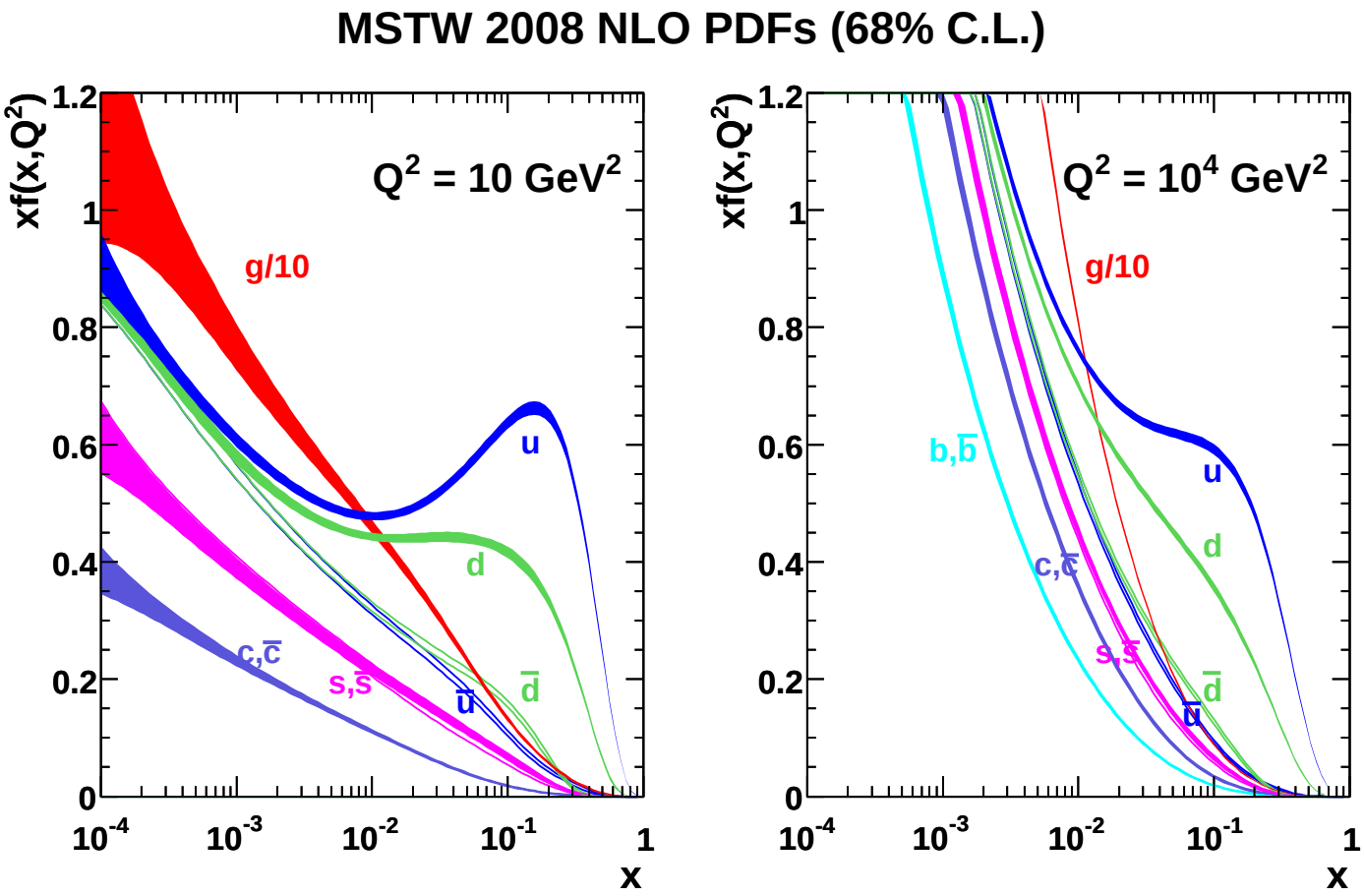

Various choices of PDF – MSTW, CTEQ, NNPDF, AB(K)M, HERA, Jimenez-Delgado *et al* *etc.*. All LHC cross-sections rely on our understanding of these partons.

Leads to very accurate and precise predictions.

Comparison of MSTW prediction for Z rapidity distribution with data.

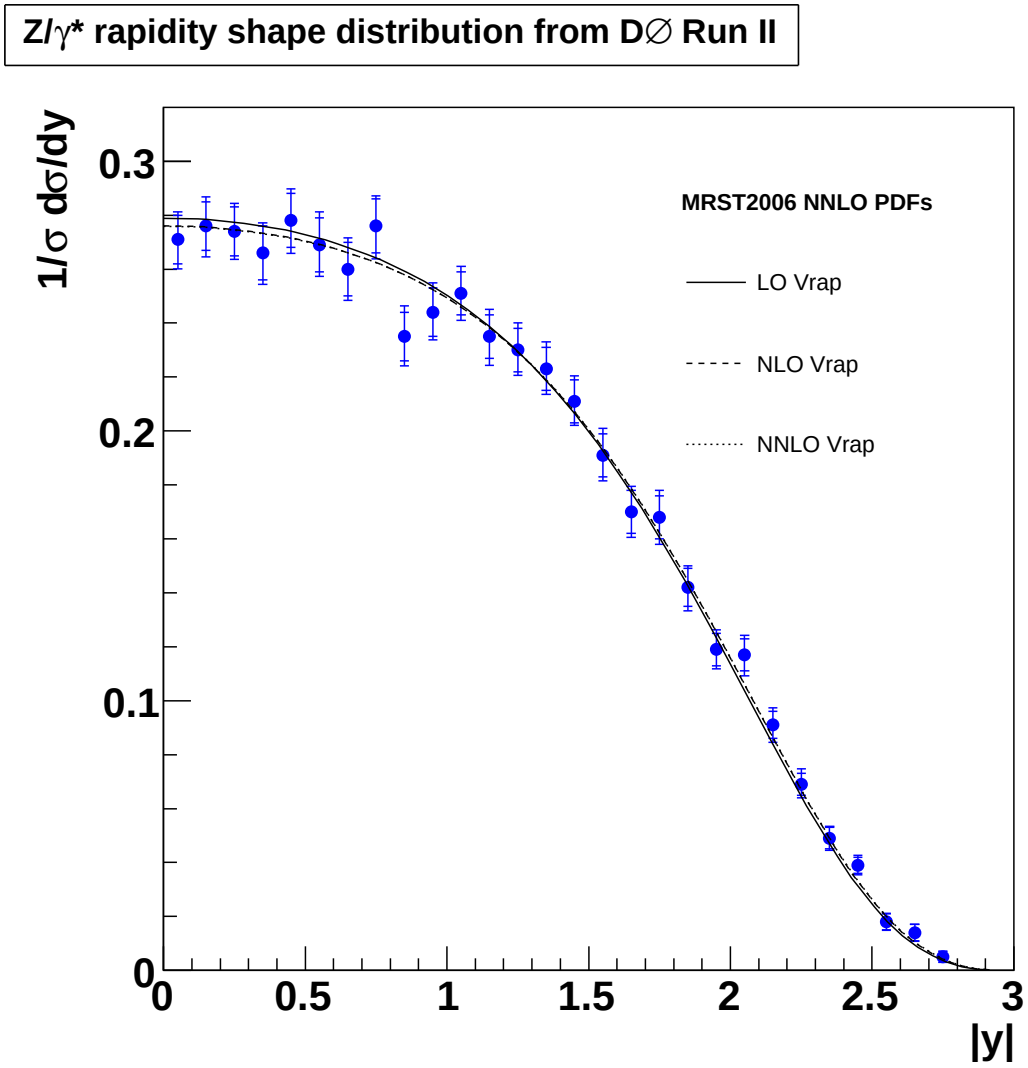

Parton Fits and Uncertainties. Two main approaches.

Parton parameterization and Hessian (Error Matrix) approach first used by H1 and ZEUS, and extended by CTEQ.

$$\chi^2 - \chi^2_{min} \equiv \Delta\chi^2 = \sum_{i,j} H_{ij}(a_i - a_i^{(0)})(a_j - a_j^{(0)})$$

The Hessian matrix H is related to the covariance matrix of the parameters by

$$C_{ij}(a) = \Delta\chi^2 (H^{-1})_{ij}.$$

We can then use the standard formula for linear error propagation.

$$(\Delta F)^2 = \Delta\chi^2 \sum_{i,j} \frac{\partial F}{\partial a_i} (H)^{-1}_{ij} \frac{\partial F}{\partial a_j},$$

This is the most common approach.

Can find and rescale eigenvectors of H leading to diagonal form

$$\Delta\chi^2 = \sum_i z_i^2$$

2-dim (i,j) rendition of d-dim (~20) PDF parameter space

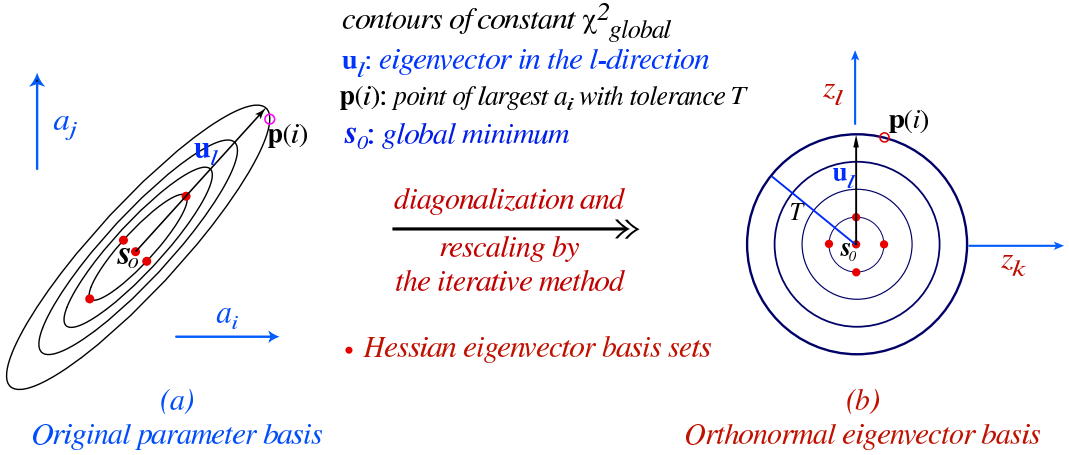

Implemented by CTEQ, then MRST/MSTW, HERAPDF. Uncertainty on physical quantity then given by

$$(\Delta F)^2 = \sum_i \left(F(S_i^{(+)}) - F(S_i^{(-)})\right)^2,$$

where $S_i^{(+)}$ and $S_i^{(-)}$ are PDF "error sets" displaced along eigenvector direction.

Must choose "correct" $\Delta\chi^2$ given complication of errors in full fit and sometimes conflicting data sets.

Neural Network group (Ball *et al.*) limit parameterization dependence. Leads to alternative approach to "best fit" and uncertainties.

First part of approach, no longer perturb about best fit.

- Generate artificial data according to distribution

$$O_i^{(art)\,(k)} = (1 + r_N^{(k)}\,\sigma_N)\left[O_i^{(exp)} + \sum_{p=1}^{N_Sys} r_p^{(k)}\,\sigma_{i,p} + r_{i,s}^{(k)}\,\sigma_s^i\right]$$

Where $r_p^{(k)}$ are random numbers following Gaussian distribution. Hence, include information about measurements and errors in distribution of $O_{i,p}^{art,(k)}$.

Fit to the data replicas obtaining PDF replicas $q_i^{(net)(k)}$ (follows Giele *et al.*)

Mean μ_O and deviation σ_O of observable O then given by

$$\mu_O = \frac{1}{N_{rep}} \sum_1^{N_{rep}} O[q_i^{(net)(k)}], \quad \sigma_O^2 = \frac{1}{N_{rep}} \sum_1^{N_{rep}} (O[q_i^{(net)(k)}] - \mu_O)^2.$$

Eliminates parameterisation dependence by using a neural net which undergoes a series of (mutations via genetic algorithm) to find the best fit. In effect is a much larger sets of parameters – ~ 37 per distribution.

Showed equivalence of replica approach to Hessian study with eigenvectors for given $\Delta\chi^2$.

However, can generate "random" PDF sets directly from parameters and variation from eigenvectors.

$$a_i(\mathcal{S}_k) = a_i^0 + \sum_{j=1}^{n} e_{ij}\left(\pm t_j^{\pm}\right)|R_{jk}|$$

$(k = 1, \ldots, N_{\mathrm{pdf}})$. Or from eigenvectors directly (see LHCb study and De Lorenzi thesis). Far quicker.

$$F(\mathcal{S}_k) = F(S_0) + \sum_j \left[F(S_j^{\pm}) - F(S_0)\right]|R_{jk}|$$

Can use in reweighting studies as NNPDF, i.e. weight "random" set by χ^2 of fit to new data set(s) to get new distribution.

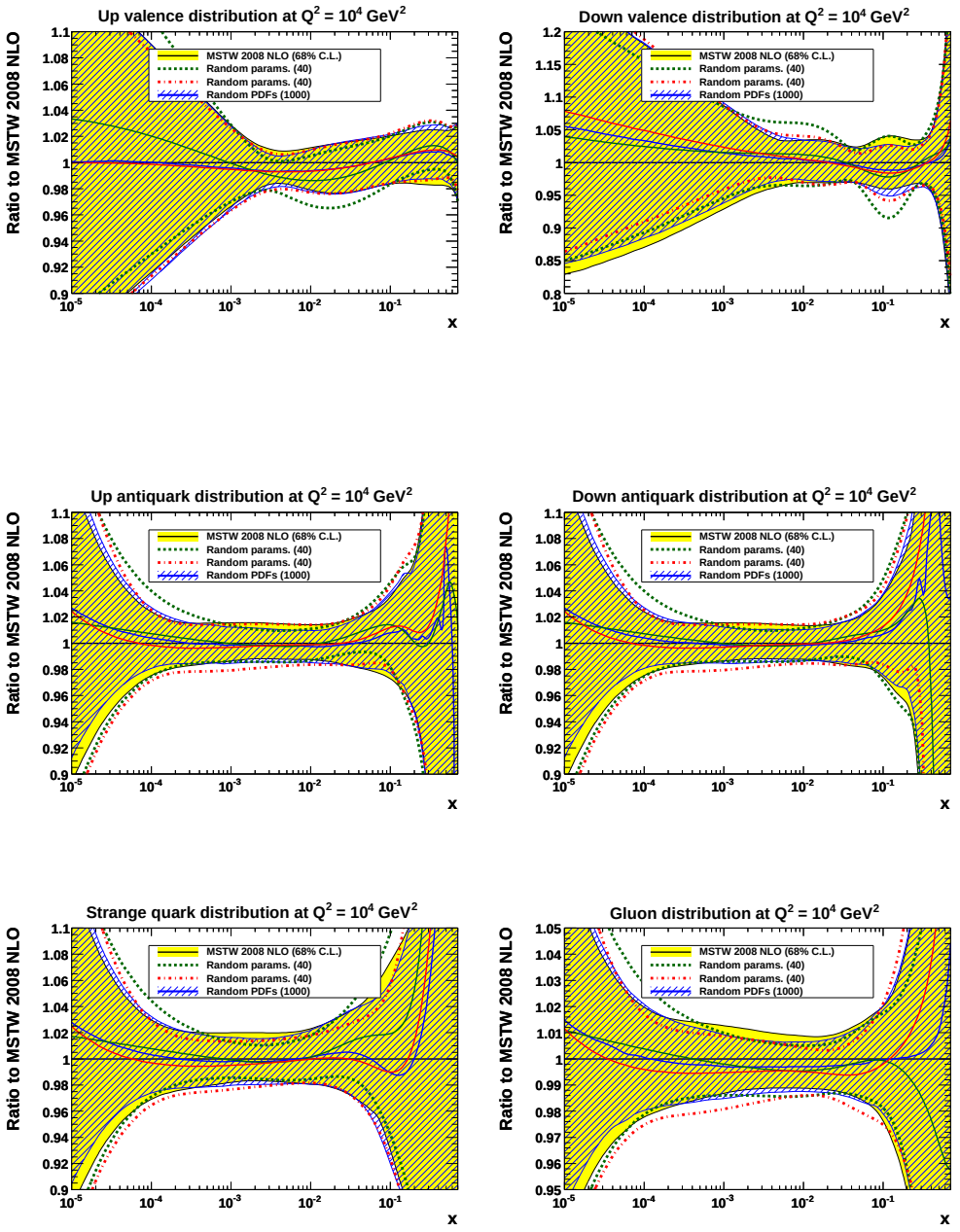

Speed of convergence of prediction for Z cross section.

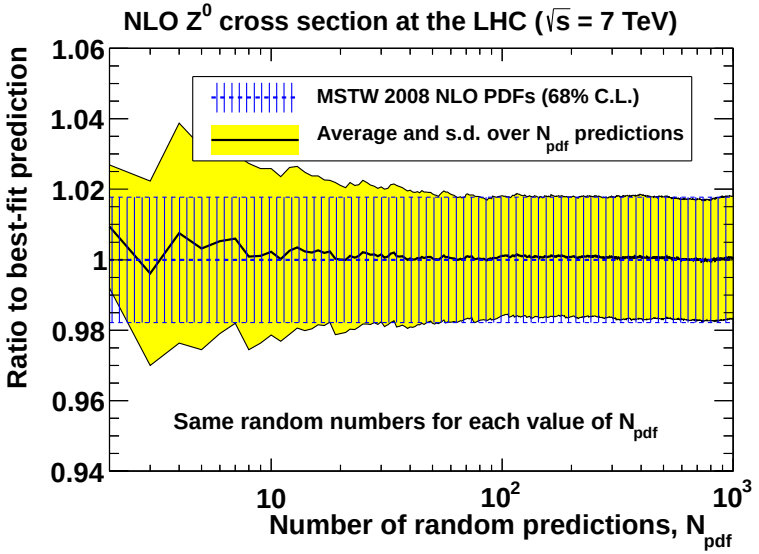

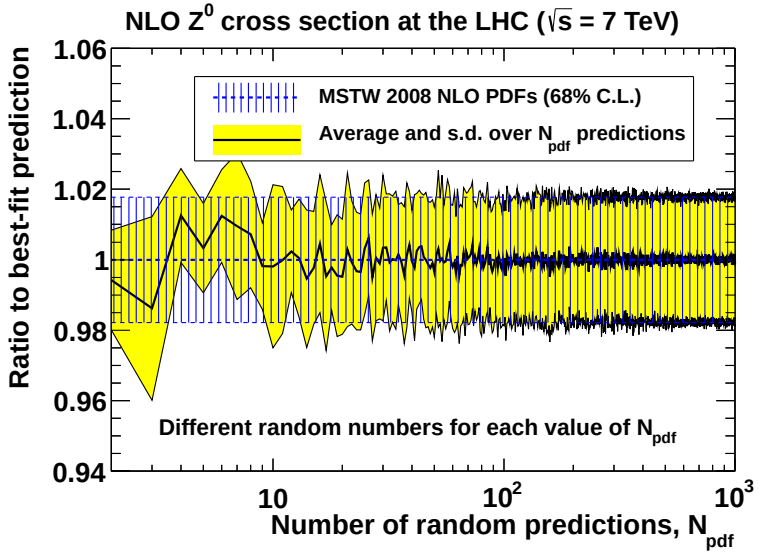

Left, add a new random set to existing ones sequentially. Right, increasing numbers of independent random sets.

Very good with 40 sets. Excellent with 100 sets.

Speed of convergence of prediction for W^+/W^- cross section ratio.

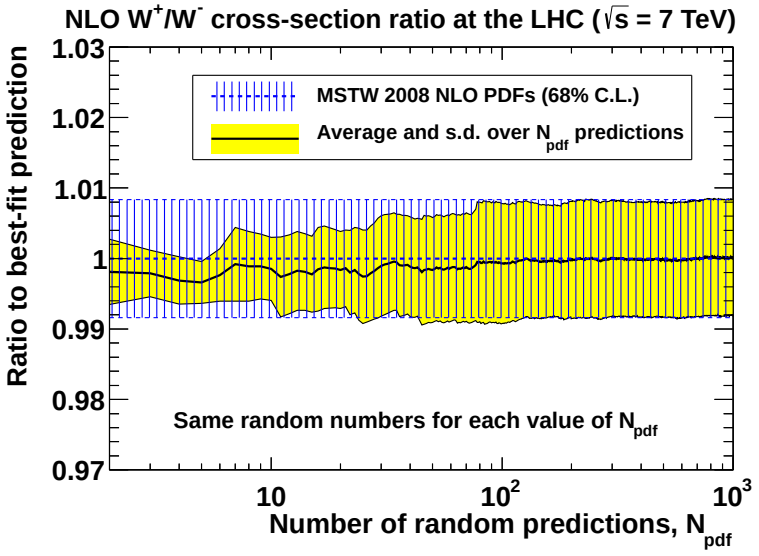

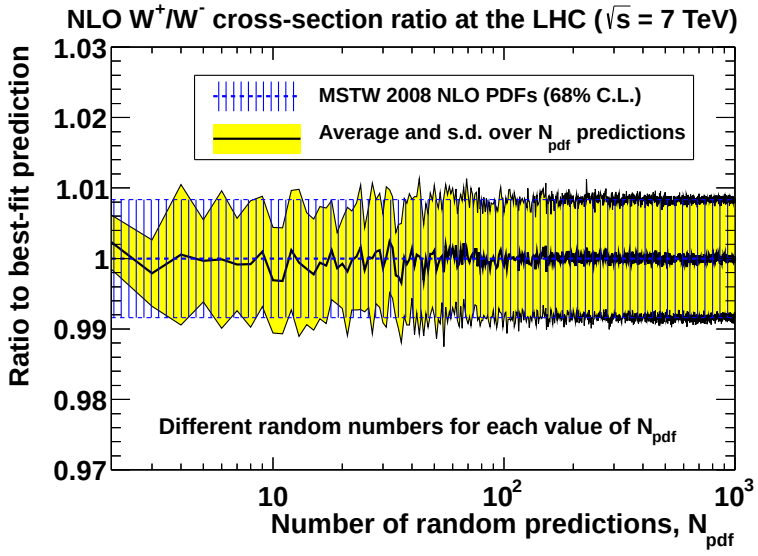

Left, add a new random set to existing ones sequentially. Right, increasing numbers of independent random sets.

Very good with 40 sets. Excellent with 100 sets.

Speed of convergence of prediction for $t\bar{t}$ cross section.

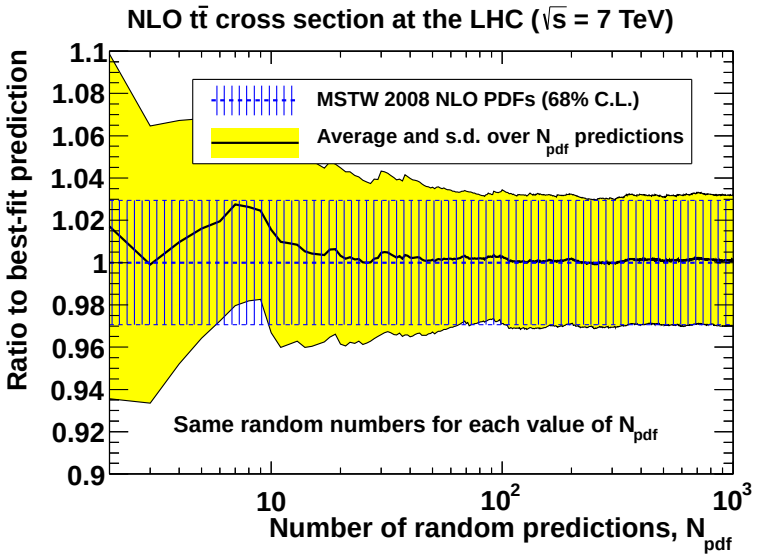

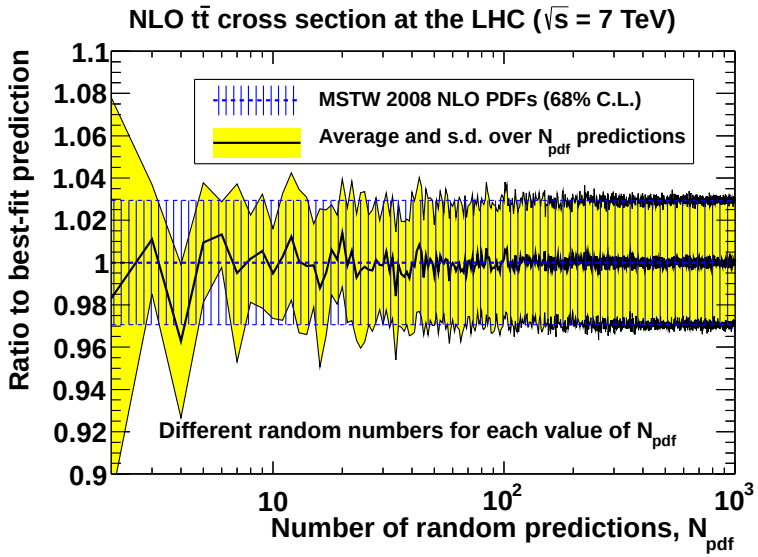

Left, add a new random set to existing ones sequentially. Right, increasing numbers of independent random sets.

Very good with 40 sets. Excellent with 100 sets.

Speed of convergence of prediction for H cross section.

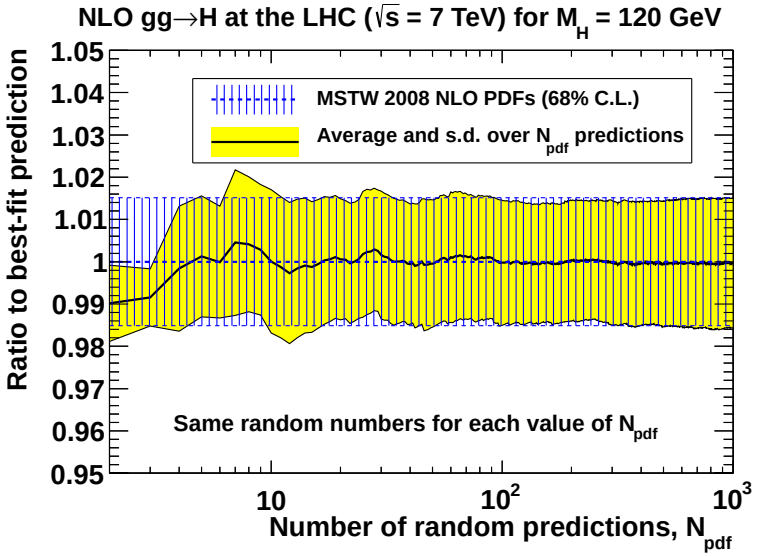

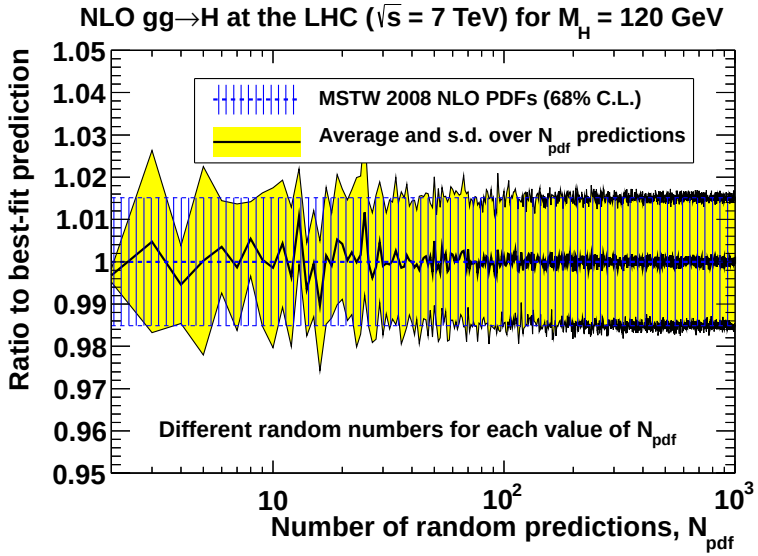

Left, add a new random set to existing ones sequentially. Right, increasing numbers of independent random sets.

Very good with 40 sets. Excellent with 100 sets.

Can combine PDF sets, e.g. comparison to PDF4LHC prescription.

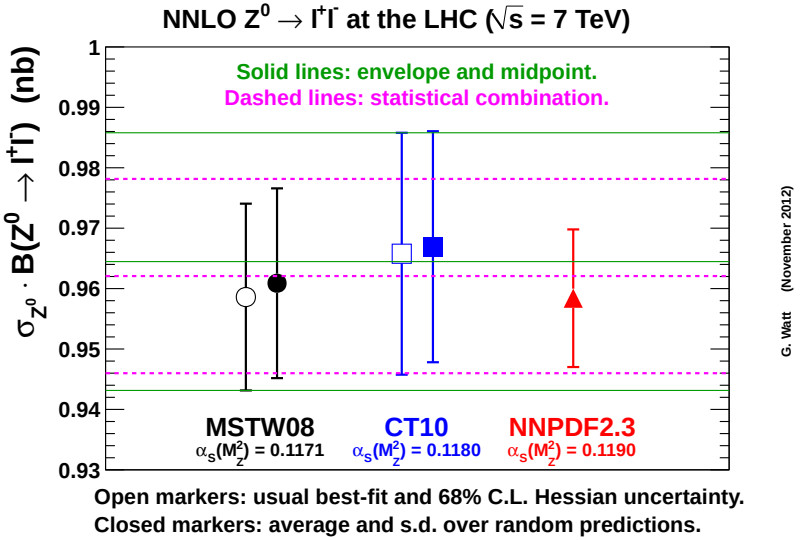

Open markers: usual best-fit and 68% C.L. Hessian uncertainty.
Closed markers: average and s.d. over random predictions.

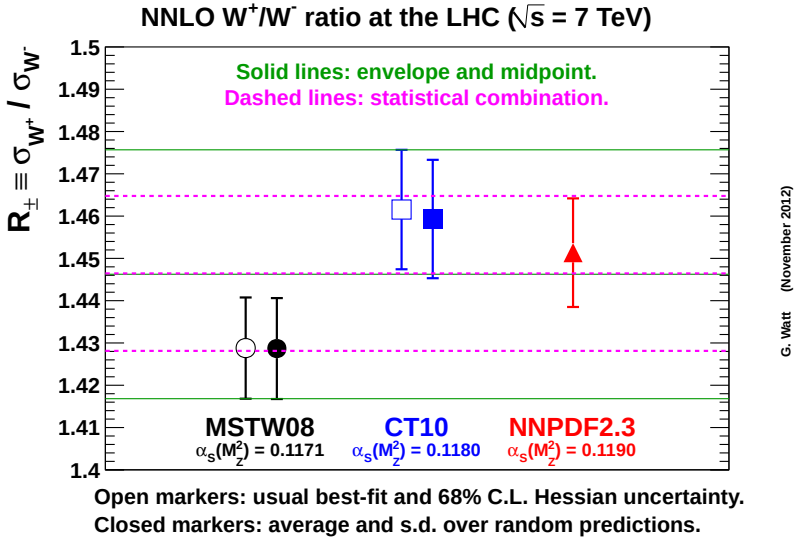

Open markers: usual best-fit and 68% C.L. Hessian uncertainty.
Closed markers: average and s.d. over random predictions.

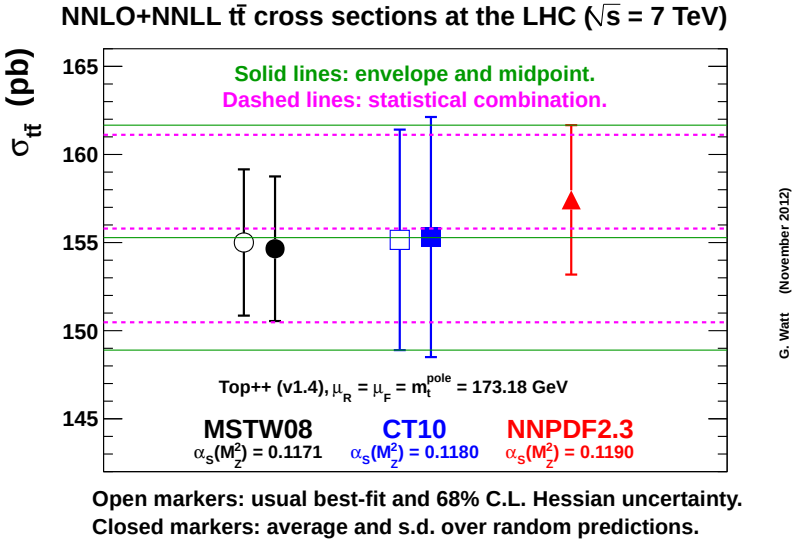

Open markers: usual best-fit and 68% C.L. Hessian uncertainty.
Closed markers: average and s.d. over random predictions.

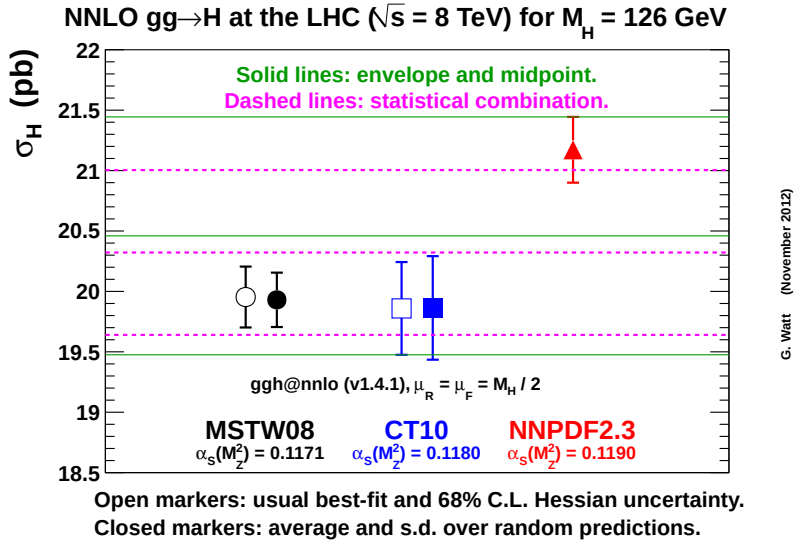

Open markers: usual best-fit and 68% C.L. Hessian uncertainty.
Closed markers: average and s.d. over random predictions.

Smaller uncertainty and shifted central value if disagreement between individual predictions. (Plots by G. Watt at http://mstwpdf.hepforge.org/random/).

Comparison to LHC data. (arXiv:1211.1215, A.D. Martin *et. al.*)

Start with ATLAS jets. Comparison clearly fine.

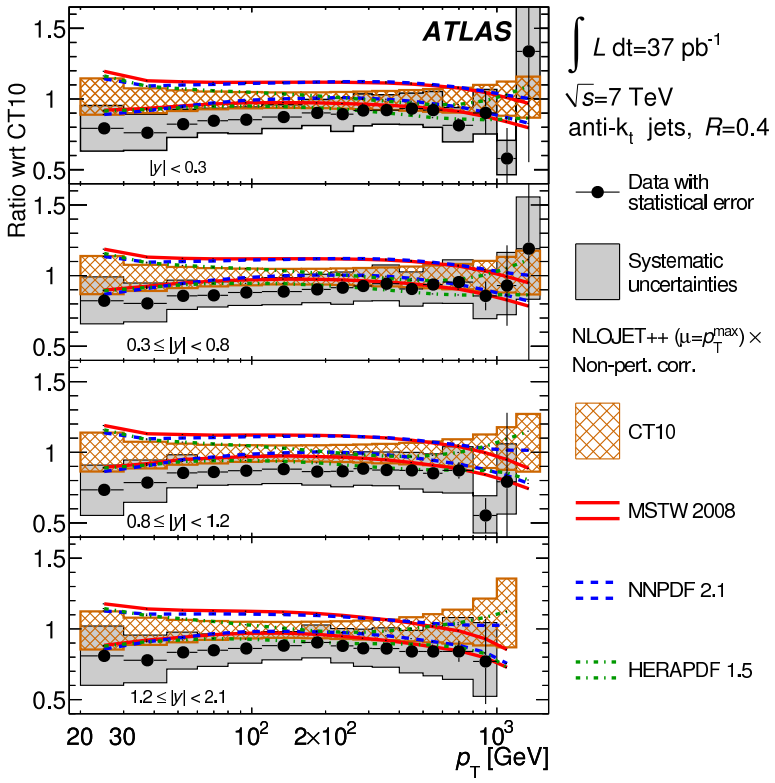

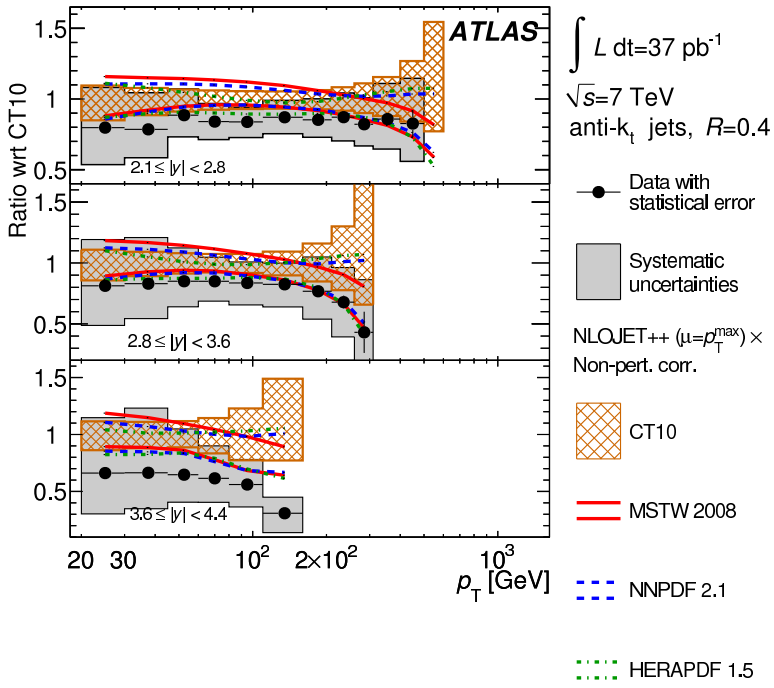

Being more quantitative Using APPLGrid or FastNLO (B. Watt).

Scale	pT/2	pT	2pT
Inclusive (R=0.4)	0.752	0.773	0.703
Inclusive (R=0.6)	0.845	0.790	0.721

MSTW fit very good, see χ^2 per point above. Always close to, and sometimes the best of any PDF set, particularly for $R = 0.6$. Not a huge variation in PDFs across groups though.

Can see effect of data on the gluon by using the reweighting technique, $R = 0.6$ ($R = 0.4$ similar). Clearly little pull with present data.

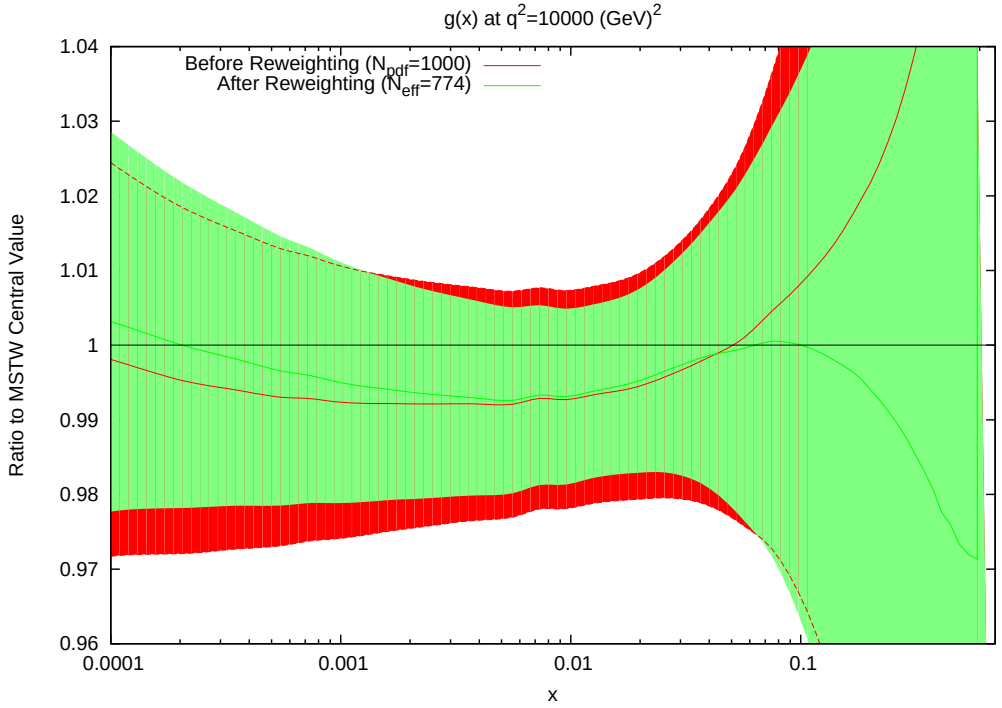

Comparison of MSTW2008 to total W, Z excellent.

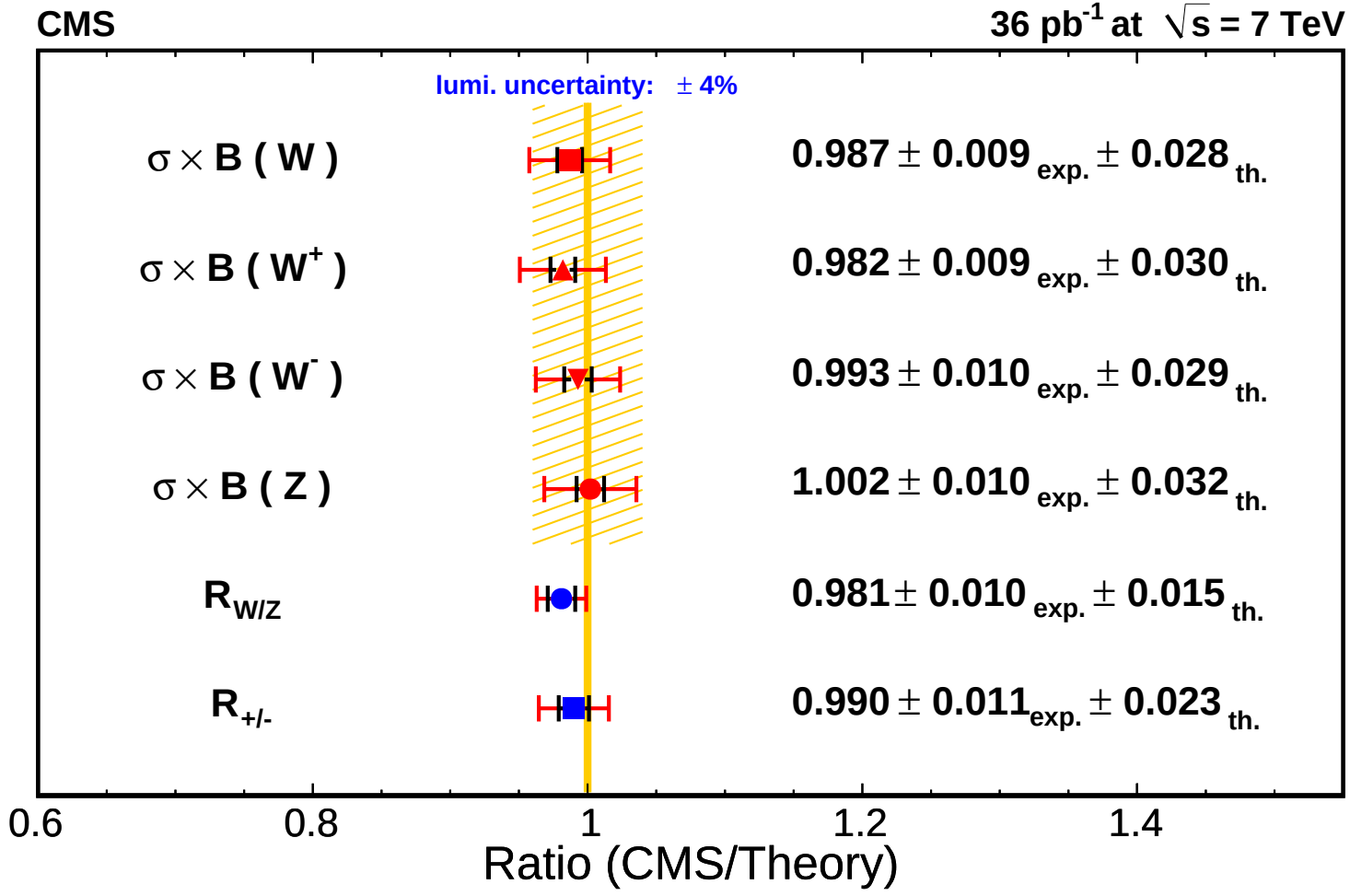

Comparisons between different sets for Inclusive predictions.

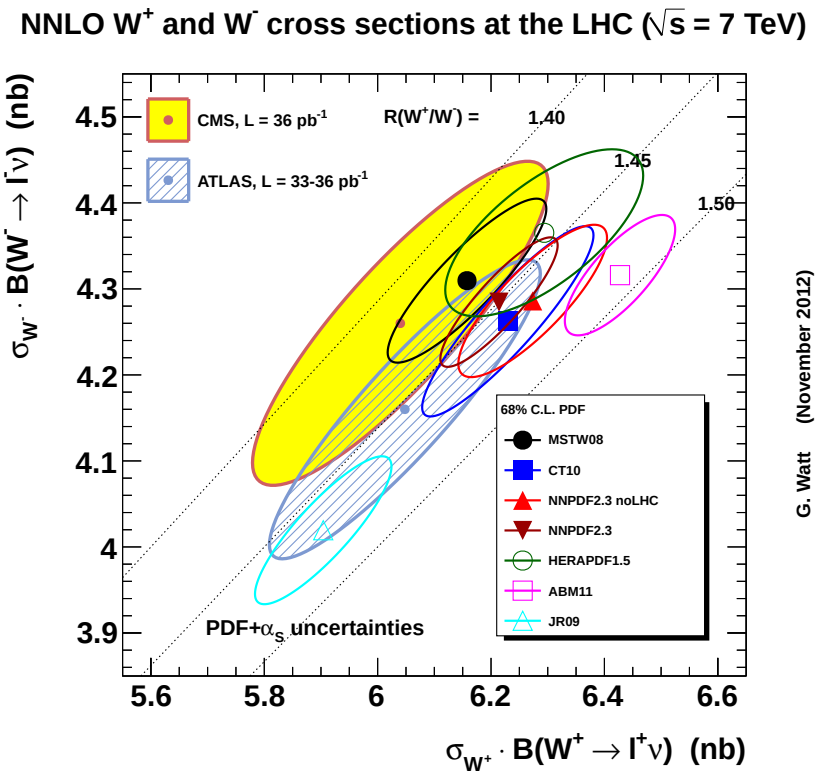

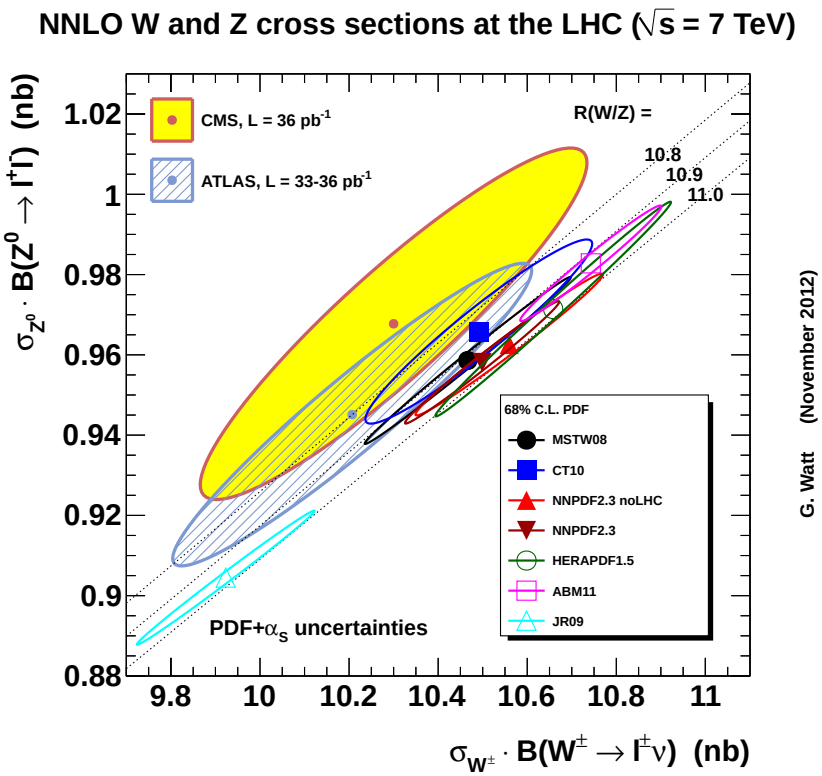

(Plots by G. Watt at http://mstwpdf.hepforge.org/pdf4lhc/AR/).

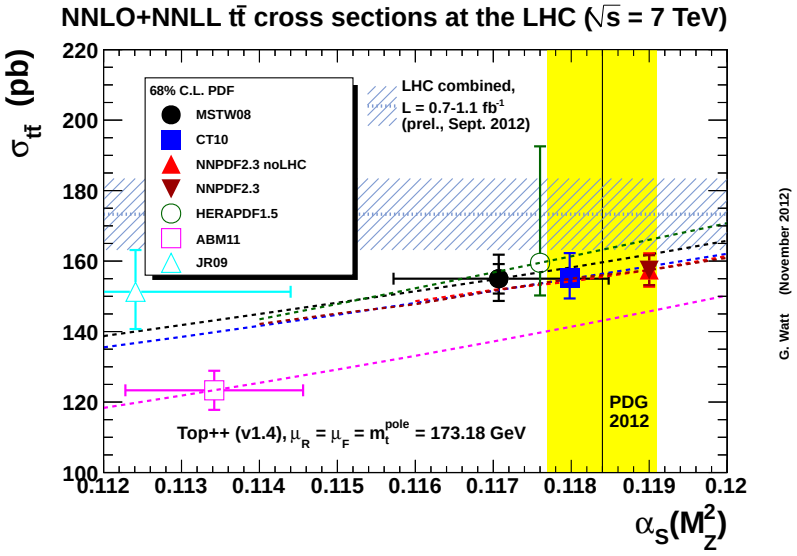

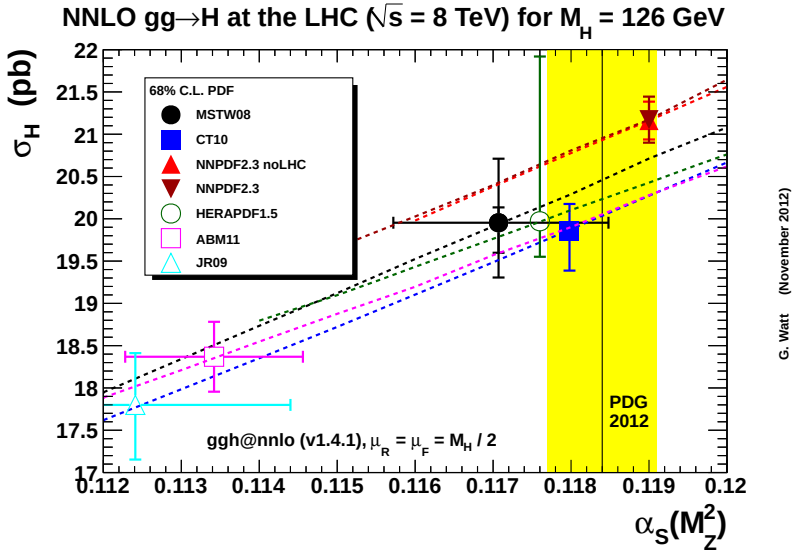

Note variety of values of $\alpha_S(M_Z^2)$ used by different groups.

Correlates with PDF luminosity plots

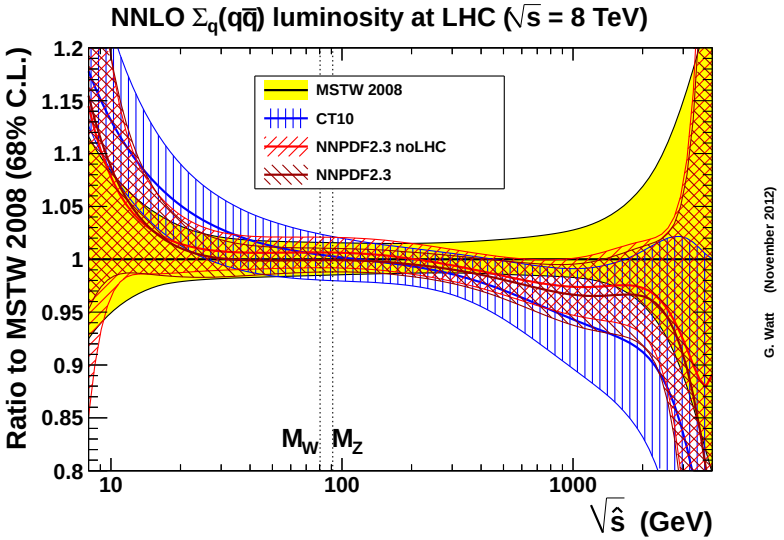

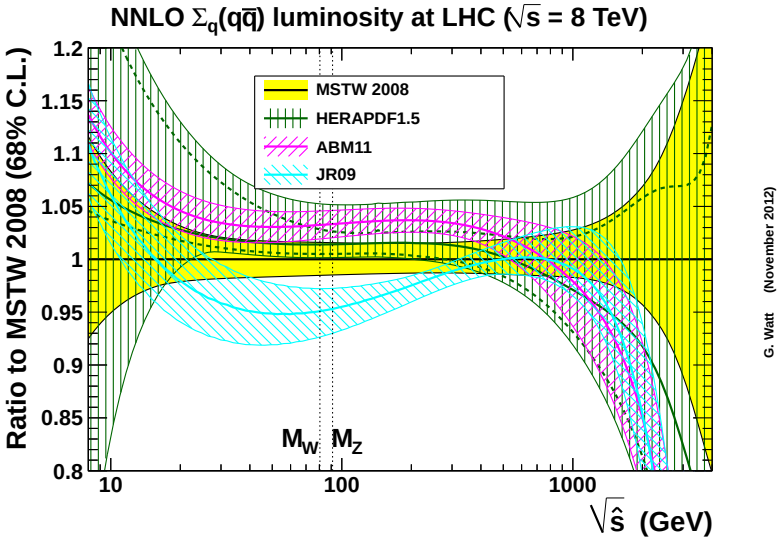

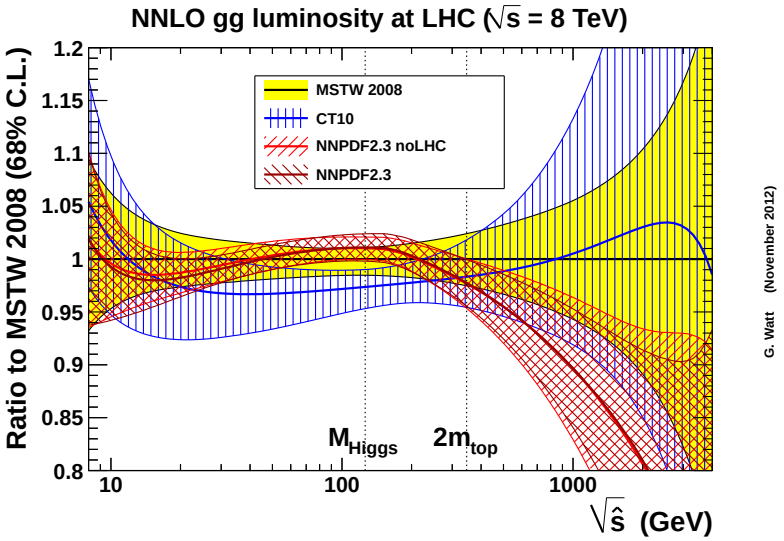

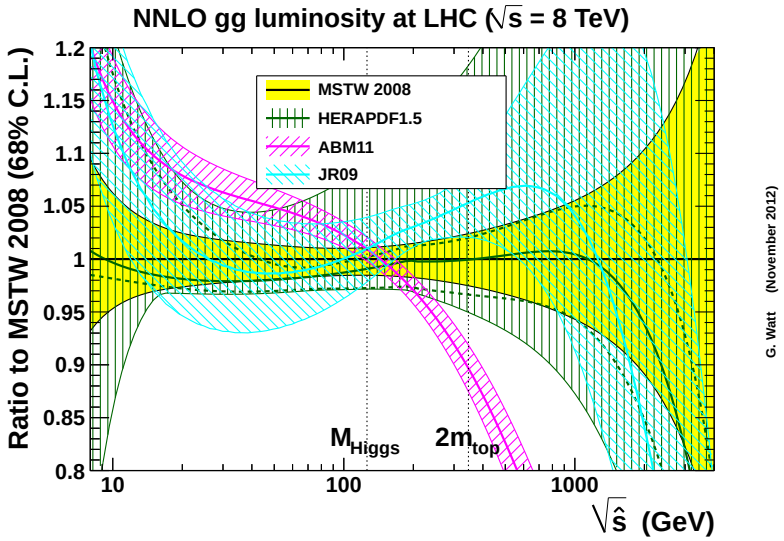

Some pretty clear difference between some of the groups. More later.

MSTW also pretty good for inclusive distributions. Except some problems with asymmetry. Comparison gives $\chi^2/N_{\rm pts} = 60/30$

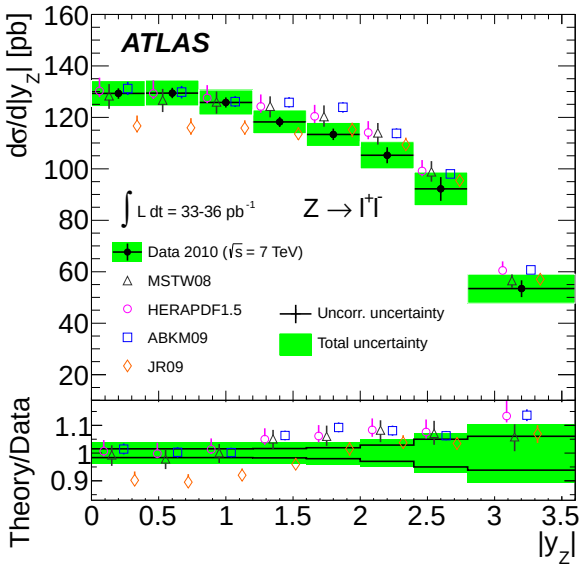

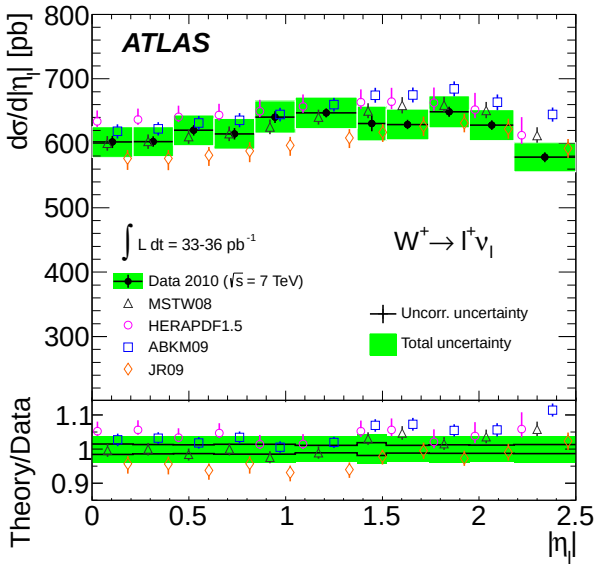

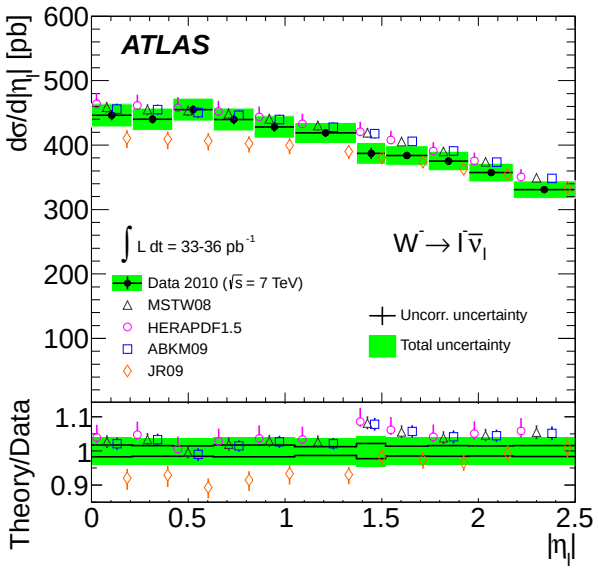

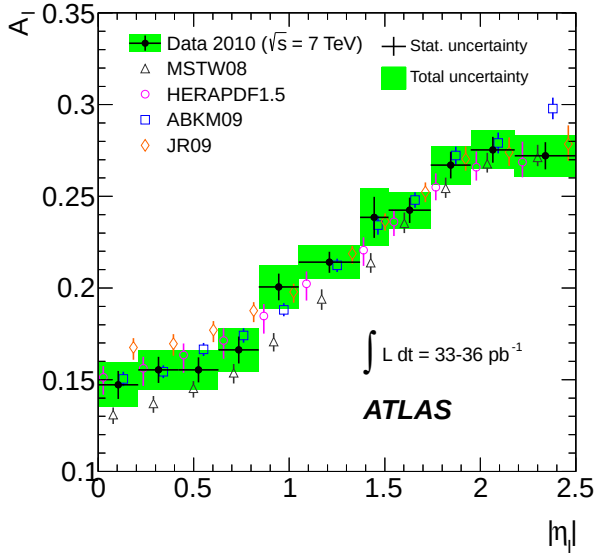

MSTW pretty good for ATLAS W, Z distributions, except some problems with asymmetry.

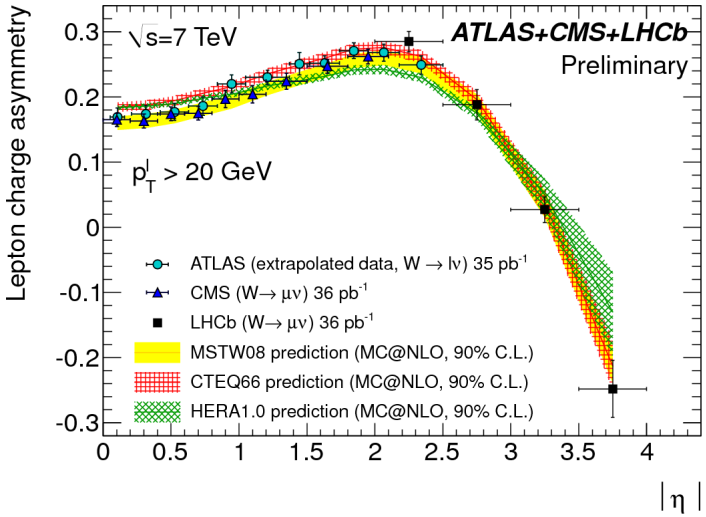

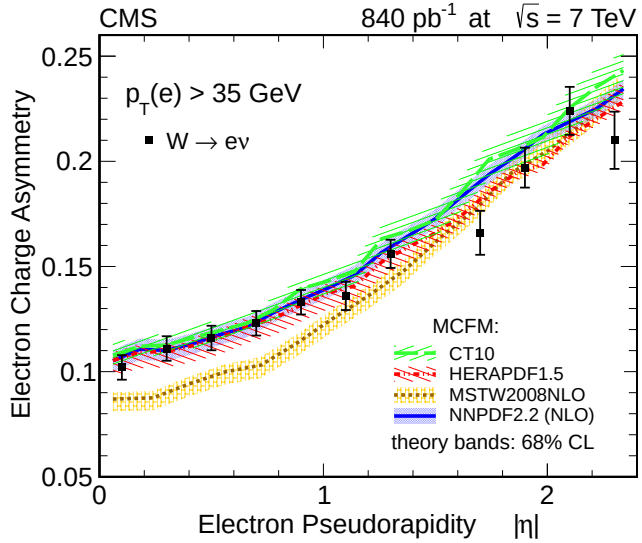

Similar for CMS data (will return to this later), though depends on p_T cut. Generally very good for LHCb.

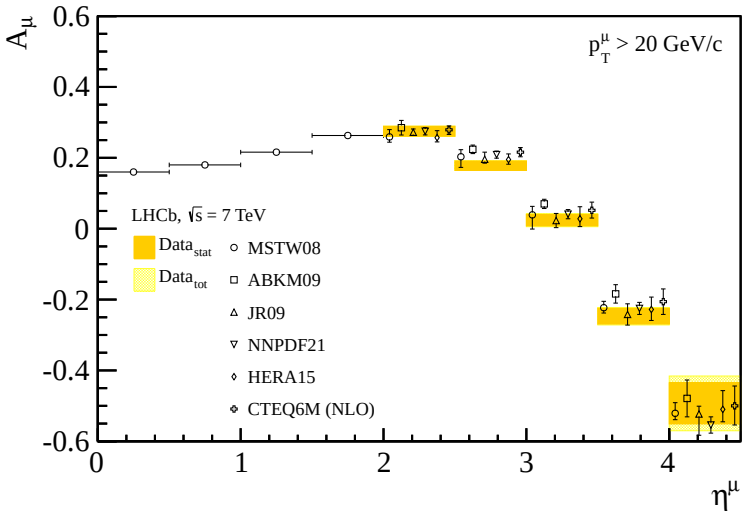

Asymmetry used (G. Watt, R.T.) in reweighting (JHEP 1208 (2012) 052), and moves $u_V - d_V$ up near $x = 0.01$ - where parameterisation perhaps underestimates uncertainty. (ATLAS left, CMS $p_T > 25\mathrm{GeV}$ right).

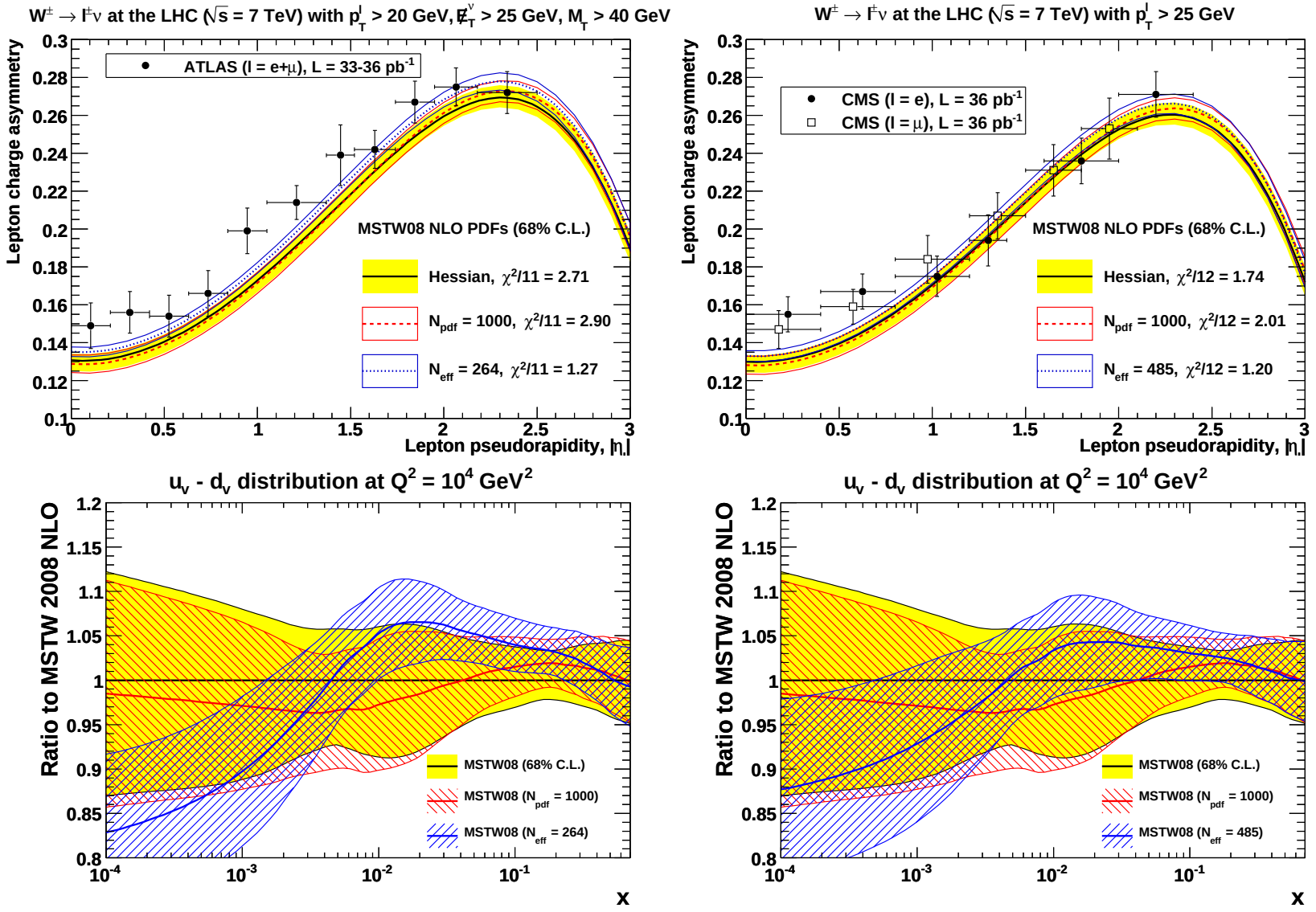

Investigation of Parameterisation Issues

In the light of Monte Carlo studies investigate parameterisation dependence, initially concentrating on valence quarks.

Decide to use Chebyshev polynomials (looked at other possibilities)

$$xf(x,Q_0^2) = A(1-x)^{\eta}x^{\delta}(1+\sum_n a_n T_n(y))$$

i.e. keep high and low x limits. Choose $y = 1-2\sqrt{x}$.

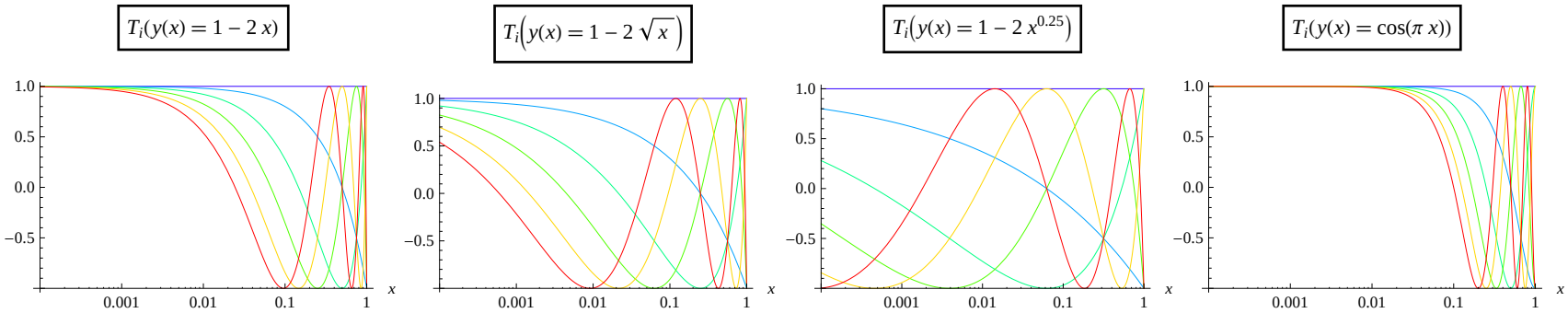

Same choice as in Pumplin study. Slightly different to Glazov, Moch and Radescu.

It is an open question how many parameters are required to accurately fit a simple shape such as that for $xu_V(x, Q^2)$ or $xd_V(x, Q^2)$.

Investigate by generating pseudo-data for various types of parton distribution using a function with very many parameters, then fitting with smaller numbers.

Fairly similar conclusion independent of type of parameterisation.

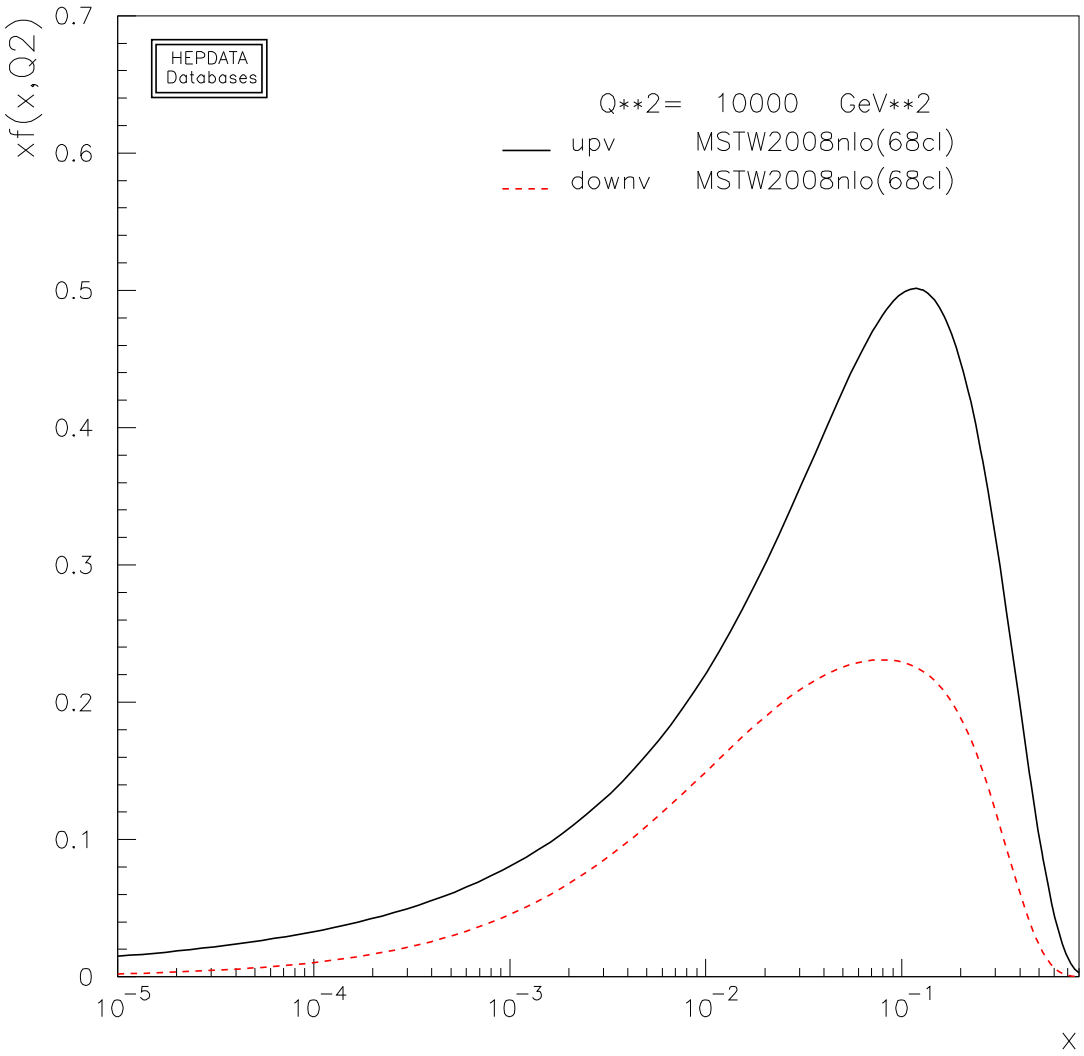

Example, fit to pseudo-data for valence quark generated between $x = 0.01$ and $x = 0.7$. For precise match to pseudo-data need 4 polynomials.

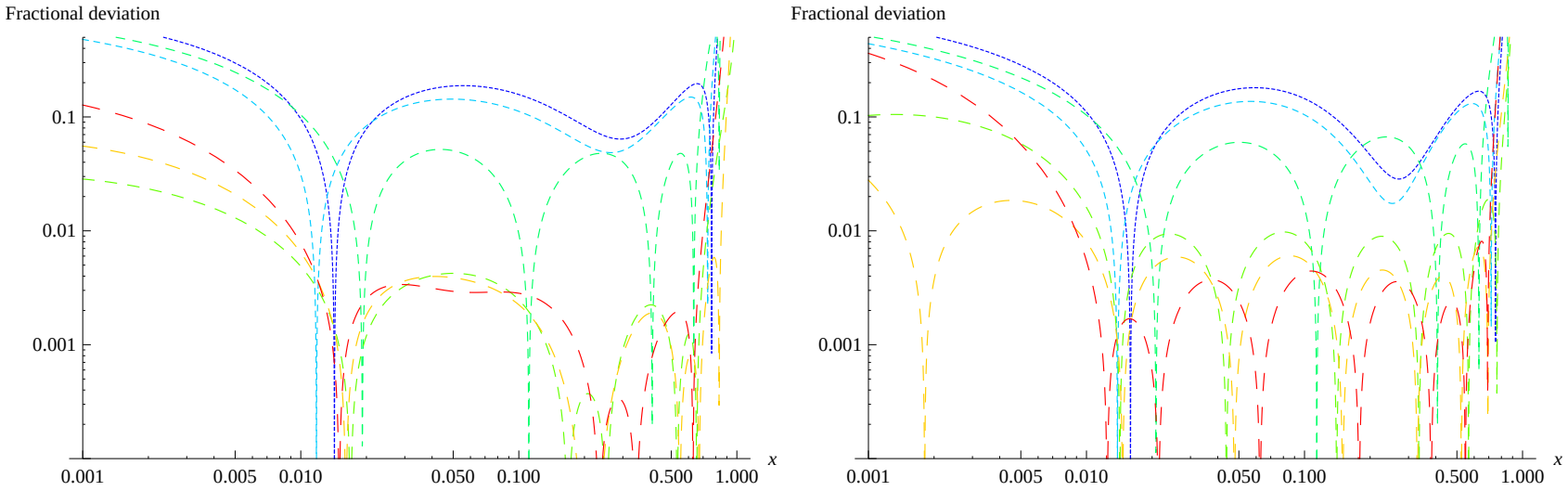

Look at χ^2 distribution with increasing terms in polynomial.

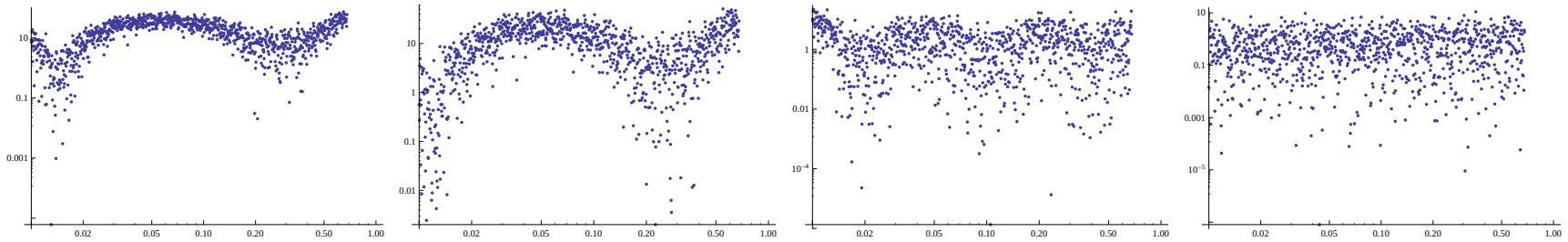

Very good fits with 4 parameters. More tends to give over-fitting and peculiarities outside of range of x fit.

Fits to same data as MSTW2008 with 2 extra parameters for valence quarks – $28 \rightarrow 32$ params.

Also with 2 extra parameters for valence quarks and sea – $28 \rightarrow 34$ params. No extra parameters in the gluon found to be necessary.

$\Delta\chi^2 = -29$, MSTW2008CP pdfs. Only real change in small-x u_V, and sea at low Q^2.

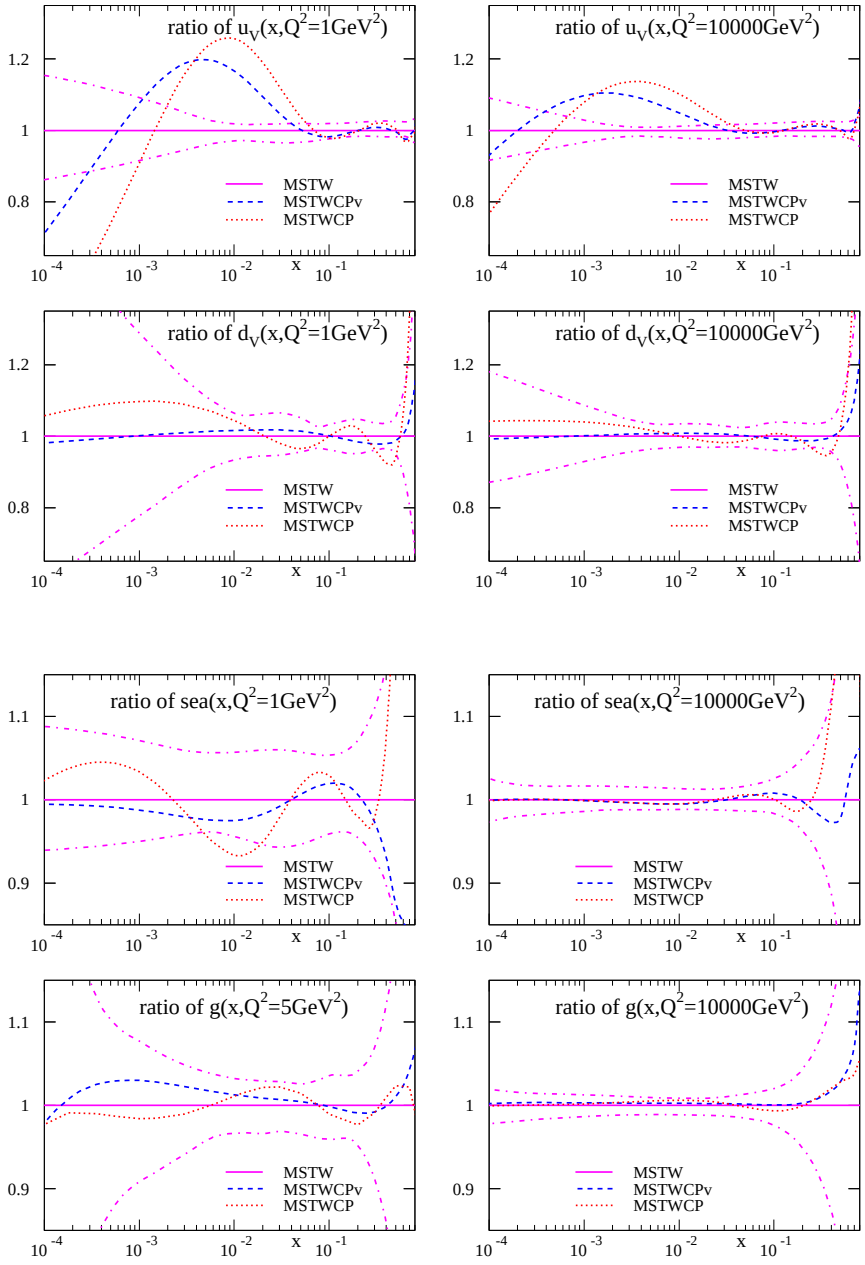

Also do the same fits with a freedom in the deuterium corrections – more stable than previous MSTW studies. MSTW2008CPdeut PDFs.

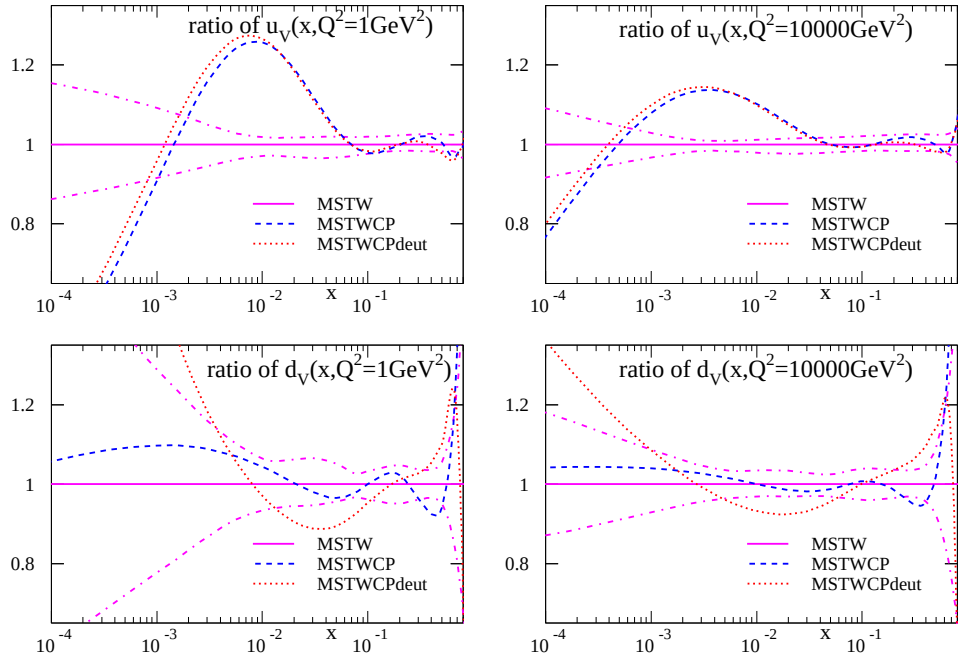

Now also get variation in $d_V(x)$ for higher x due to deuterium correction (seen before) and $x \leq 0.03$ due to parameterization and corrections.

Fit to ATLAS W, Z rapidity data at NLO improves to $49/30$ for MSTWCP and $46/30$ for MSTWCPdeut.

Shown is change in central value and uncertainty for $u_V(x) - d_V(x)$ at $Q^2 = 10,000\ \mathrm{GeV}^2$.

Biggest effect at lower x than probed at the LHC (yet).

Uncertainty sets have 23 eigenvectors (20 in MSTW2008).

Main effect in uncertainty an increase in $d_V(x, Q^2)$ due to deuterium correction uncertainties, and minor valence uncertainty increase from extra parameter.

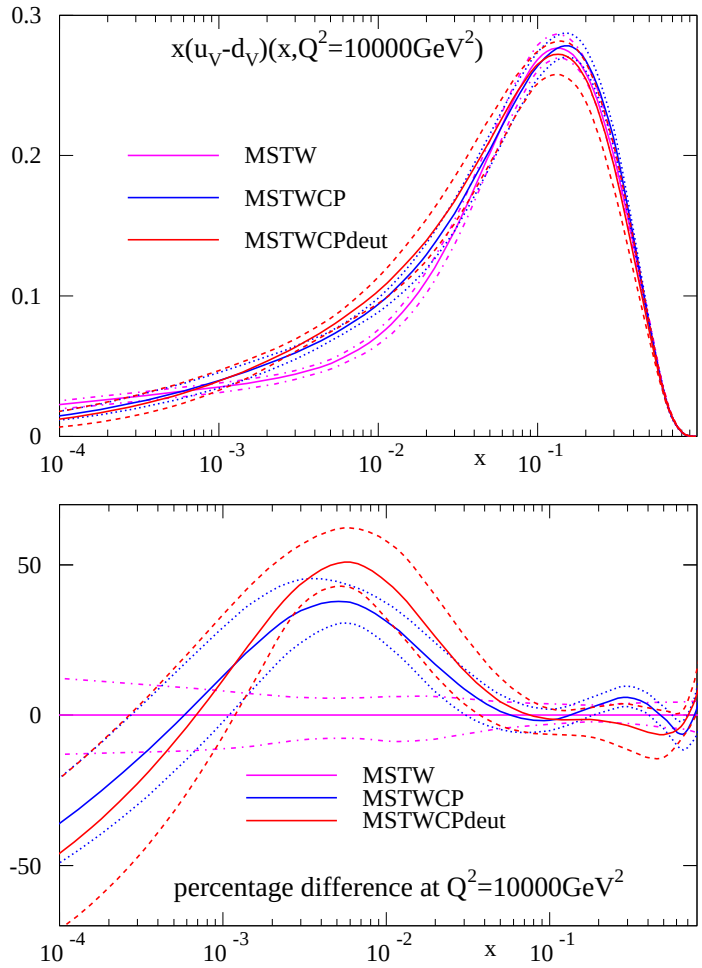

Increases lepton asymmetry, but very preferentially for high p_T cut. (Curves made here with LO calculations).

Most of the effect already obtained for parameterisation extension, but some from deuterium study.

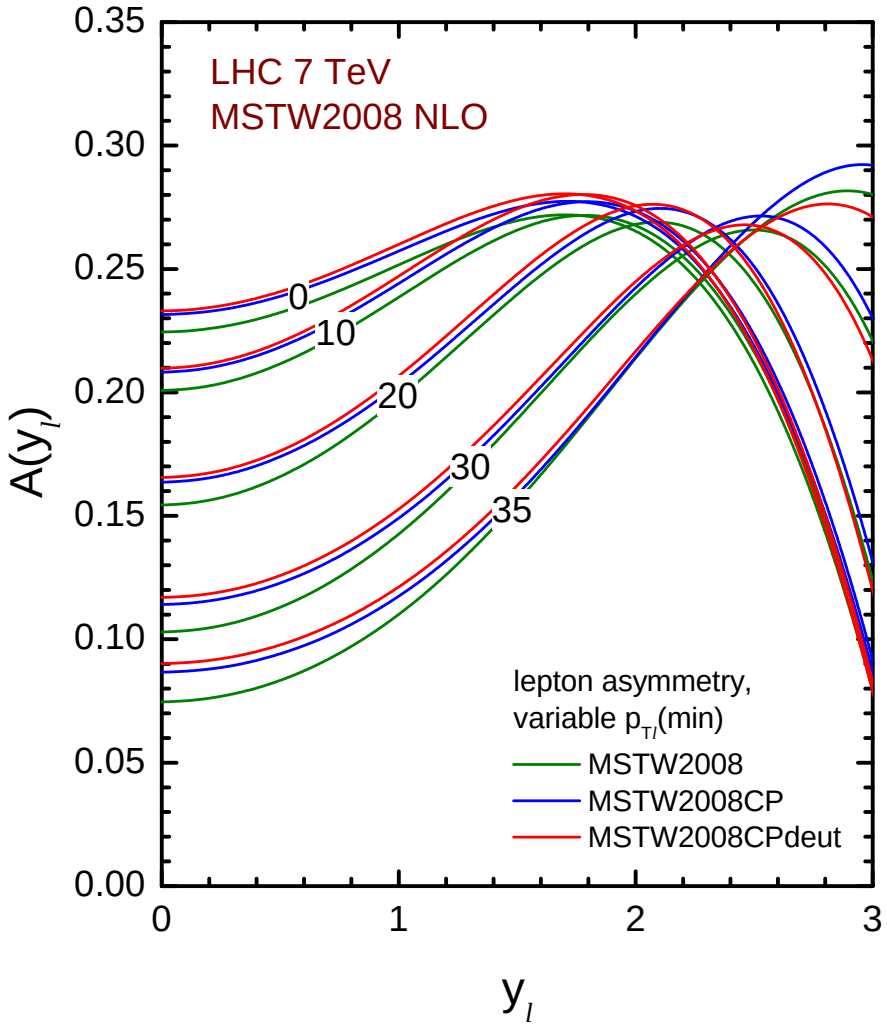

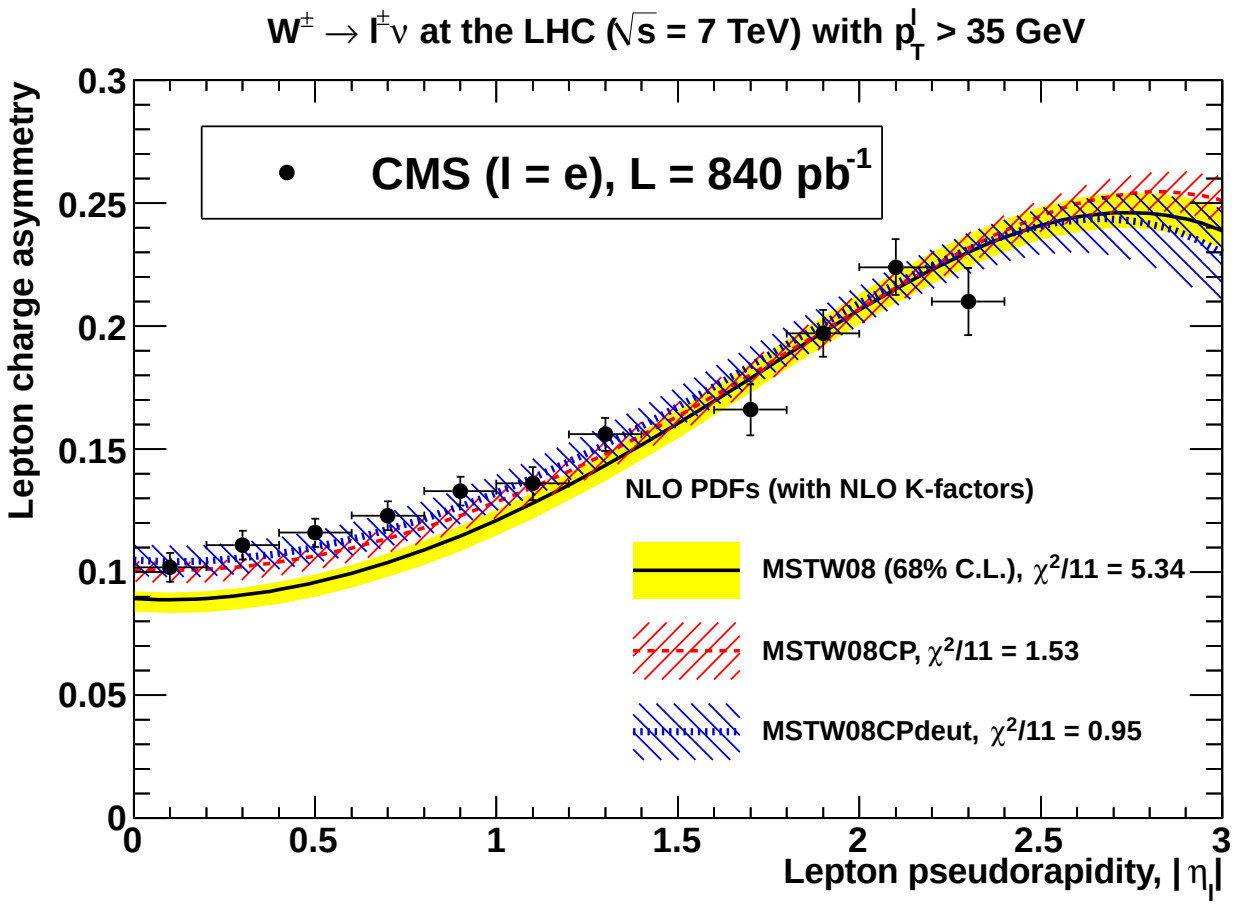

Prediction for $p_T > 35\mathrm{GeV}$ CMS asymmetry data.

Note no change to data fit, just parameterisation and some from deuterium corrections.

Main deuterium effect absence of shadowing used in default fit.

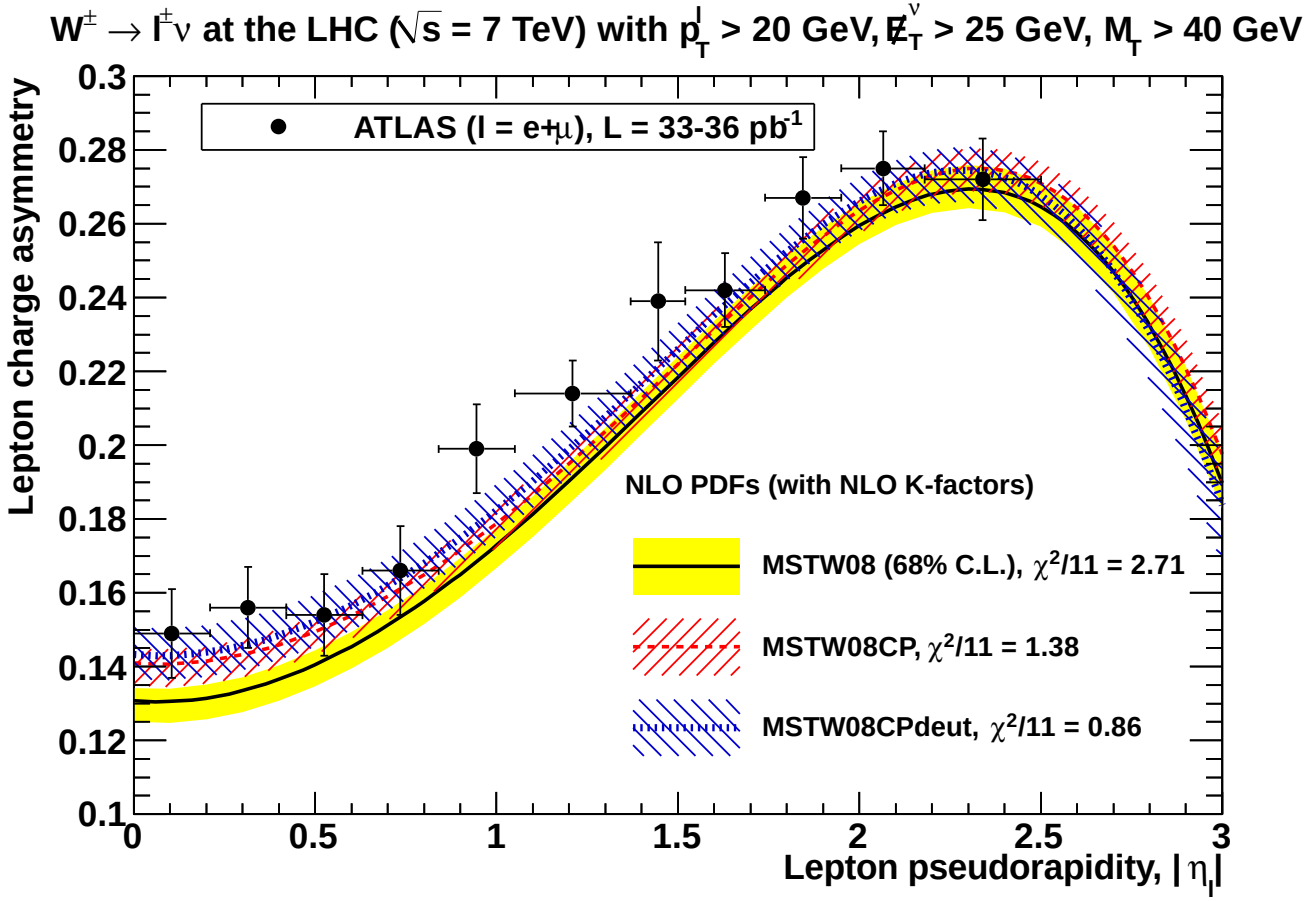

Prediction for ATLAS asymmetry data.

Note no change to data fit, just parameterisation and some from deuterium corrections.

Big change in high-p_T cut asymmetry, but this is very specifically sensitive to $u_V(x, Q^2) - d_V(x, Q^2)$.

What about other quantities?

Other PDFs changed little. α_S free but tiny change. Expect little variation.

Seen clearly on luminosity plots (G. Watt).

A not totally insignificant change in the high-x gluon luminosity for the MSTWCPdeut set . Due to softer d_V

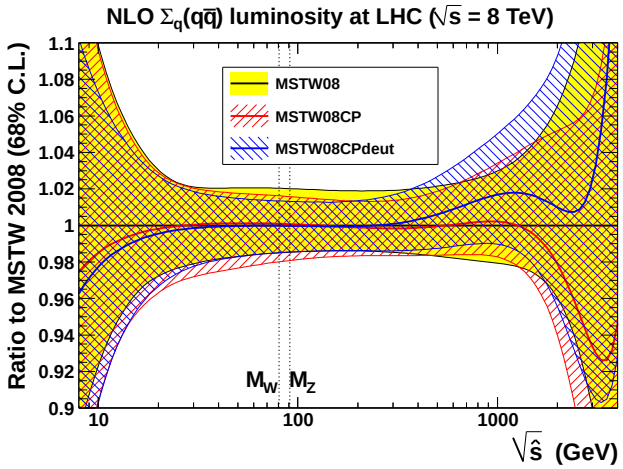

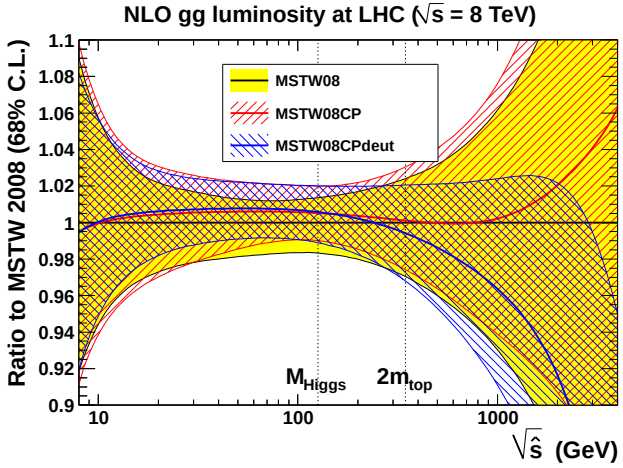

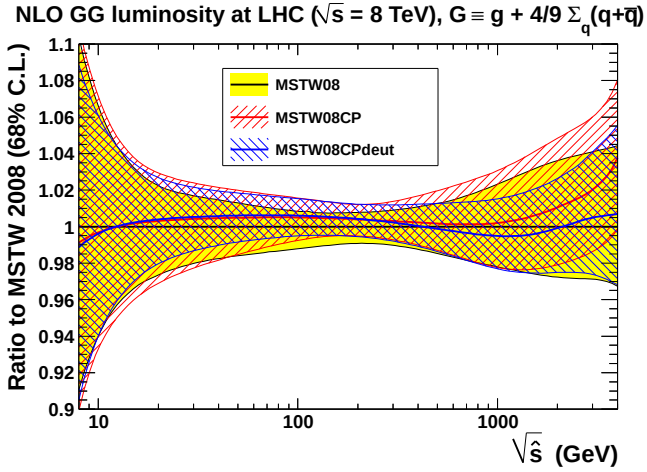

The percentage change of various cross sections due to the modifications of the MSTW2008 PDFs. In order to demonstrate the small changes in the cross sections, we also show, in the final column, the symmetrized PDF $+ \alpha_S(M_Z^2)$ percentage uncertainties for MSTW2008 PDFs.

	CP	CPdeut	unc.
W Tevatron (1.96 TeV)	+0.6	+0.1	1.8
Z Tevatron (1.96 TeV)	+0.8	+0.7	1.9
W^+ LHC (7 TeV)	+0.7	+0.3	2.2
W^- LHC (7 TeV)	−0.7	−0.4	2.2
Z LHC (7 TeV)	+0.0	−0.1	2.2
W^+ LHC (14 TeV)	+0.6	+0.3	2.4
W^- LHC (14 TeV)	−0.6	−0.5	2.4
Z LHC (14 TeV)	+0.1	−0.1	2.4
Higgs Tevatron	−0.5	−1.8	5.1
Higgs LHC (7 TeV)	+0.2	−0.1	3.3
Higgs LHC (14 TeV)	+0.1	+0.1	3.1
$t\bar{t}$ Tevatron	+0.5	−0.6	3.2
$t\bar{t}$ LHC (7 TeV)	−0.4	−1.8	3.9
$t\bar{t}$ LHC (14 TeV)	−0.2	−0.8	3.1

Can see variation of cross sections with energy.

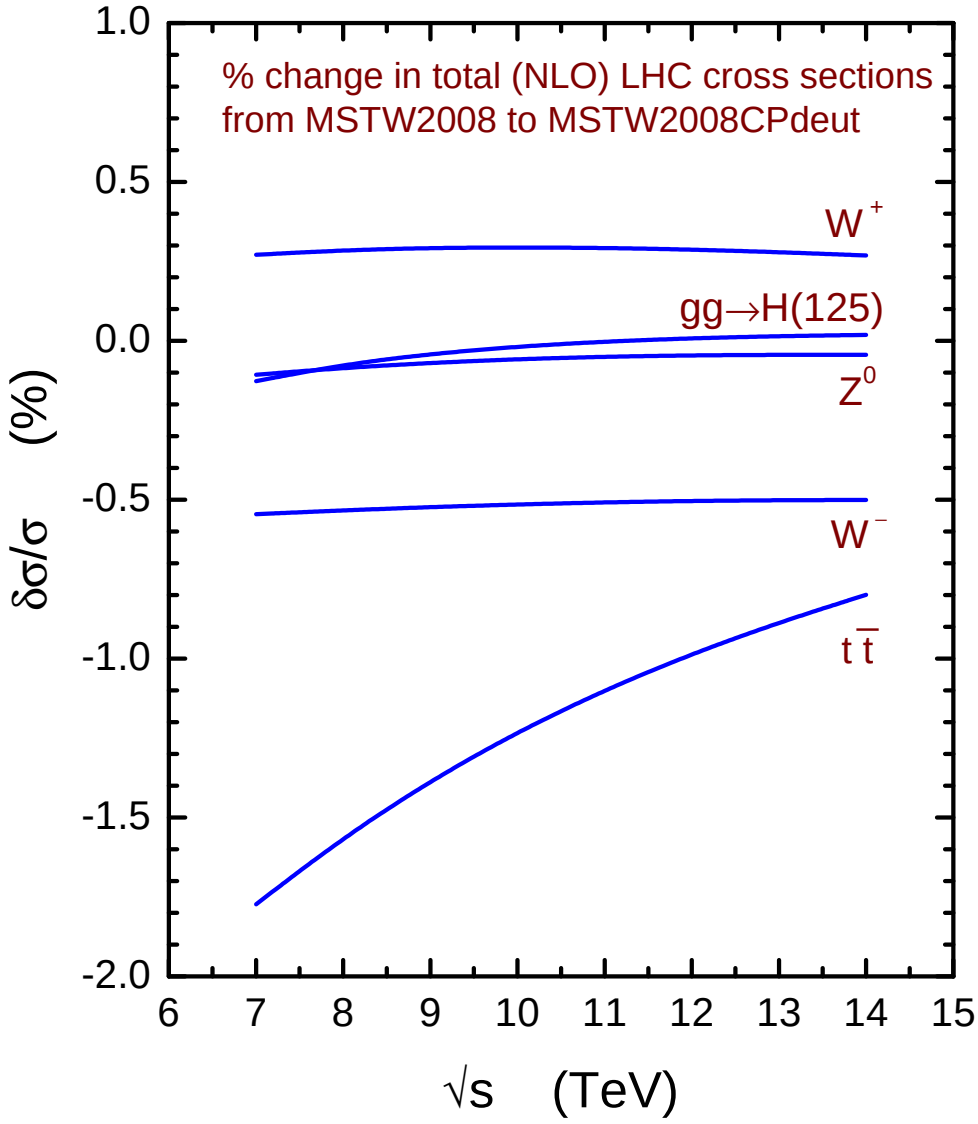

Choices for Heavy Flavours in DIS. (Extension of work in by RT in Phys.Rev. D86 (2012) 074017.)

Near threshold $Q^2 \sim m_H^2$ massive quarks not partons. Created in final state.

Described using **Fixed Flavour Number Scheme** (FFNS).

$$F(x,Q^2) = C_k^{FF,n_f}(Q^2/m_H^2) \otimes f_k^{n_f}(Q^2)$$

Does not sum $\alpha_S^n \ln^n Q^2/m_H^2$ terms in perturbative expansion. Usually achieved by definition of heavy flavour parton distributions and solution of evolution equations.

Additional problem FFNS known up to NLO (Laenen *et al.*), but are not fully known at NNLO – $\alpha_S^3 C_{2,Hi}^{FF,3}$ unknown.

Approximations based on some or all of threshold, low-x and high-Q^2 limits can be derived, see Kawamura, *et al.*,, and are sometimes used in fits, e.g. ABM11 and MSTW (at low Q^2). Generally not large except at threshold and very low x.

Variable Flavour - at high scales $Q^2 \gg m_H^2$ heavy quarks behave like massless partons. Sum $\ln(Q^2/m_H^2)$ terms via evolution. **Zero Mass Variable Flavour Number Scheme** (ZM-VFNS). Ignores $\mathcal{O}(m_H^2/Q^2)$ corrections.

$$F(x,Q^2) = C_j^{ZM,n_f} \otimes f_j^{n_f}(Q^2).$$

Partons in different number regions related to each other perturbatively.

$$f_j^{n_f+1}(Q^2) = A_{jk}(Q^2/m_H^2) \otimes f_k^{n_f}(Q^2),$$

Perturbative matrix elements $A_{jk}(Q^2/m_H^2)$ (Buza *et al.*) containing $\ln(Q^2/m_H^2)$ terms relate $f_i^{n_f}(Q^2)$ and $f_i^{n_f+1}(Q^2) \rightarrow$ correct evolution for both.

Want a **General-Mass Variable Flavour Number Scheme** (VFNS) taking one from the two well-defined limits of $Q^2 \leq m_H^2$ and $Q^2 \gg m_H^2$.

The GM-VFNS can be defined by demanding equivalence of the n_f light flavour and n_f+1 light flavour descriptions at all orders – above transition point $n_f \to n_f+1$

$$F(x,Q^2) = C_k^{FF,n_f}(Q^2/m_H^2) \otimes f_k^{n_f}(Q^2) = C_j^{VF,n_f+1}(Q^2/m_H^2) \otimes f_j^{n_f+1}(Q^2)$$
$$\equiv C_j^{VF,n_f+1}(Q^2/m_H^2) \otimes A_{jk}(Q^2/m_H^2) \otimes f_k^{n_f}(Q^2).$$

Hence, the VFNS coefficient functions satisfy

$$C_k^{FF,n_f}(Q^2/m_H^2) = C_j^{VF,n_f+1}(Q^2/m_H^2) \otimes A_{jk}(Q^2/m_H^2),$$

which at $\mathcal{O}(\alpha_S)$ gives

$$C_{2,Hg}^{FF,n_f,(1)}(\tfrac{Q^2}{m_H^2}) = C_{2,HH}^{VF,n_f+1,(0)}(\tfrac{Q^2}{m_H^2}) \otimes P_{qg}^0 \ln(Q^2/m_H^2) + C_{2,Hg}^{VF,n_f+1,(1)}(\tfrac{Q^2}{m_H^2}),$$

The VFNS coefficient functions tend to massless limits as $Q^2/m_H^2 \to \infty$.

However, $C_j^{VF}(Q^2/m_H^2)$ only uniquely defined in this limit.

Can swap $\mathcal{O}(m_H^2/Q^2)$ terms between $C_{2,HH}^{VF,0}(Q^2/m_H^2)$ and $C_{2,g}^{VF,1}(Q^2/m_H^2)$, i.e. get scheme variations.

Difference between FFNS and GM-VFNS

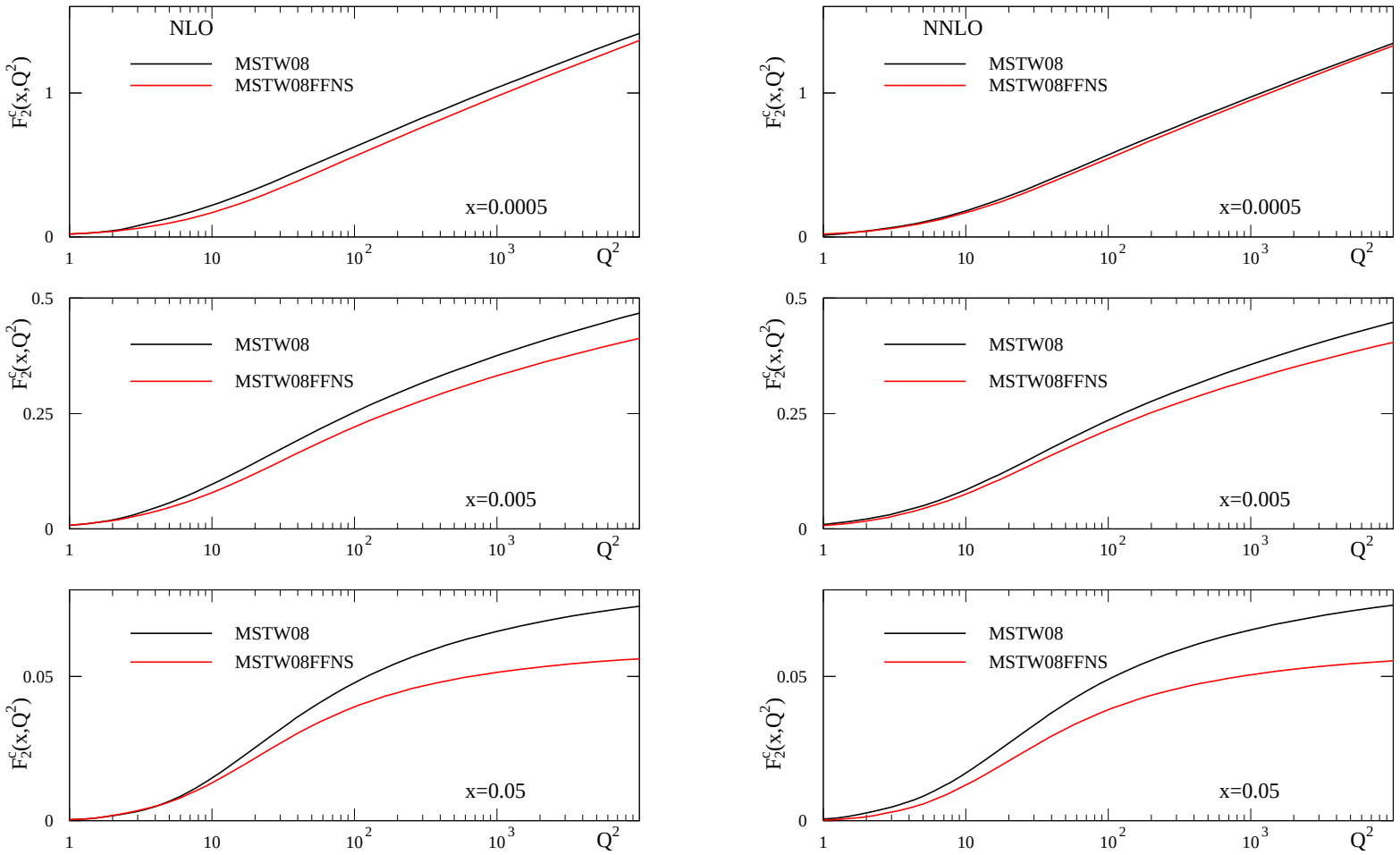

As seen at higher Q^2 charm structure function for FFNS nearly always lower than any GM-VFNS. NNLO uses $\mathcal{O}(\alpha_S^2)$ coefficient functions for $F_2^c(x,Q^2)$. Approx. $\mathcal{O}(\alpha_S^3)$ raises slightly $F_2^c(x,Q^2)$ at higher x and lowers it at small x (except very small x at low Q^2).

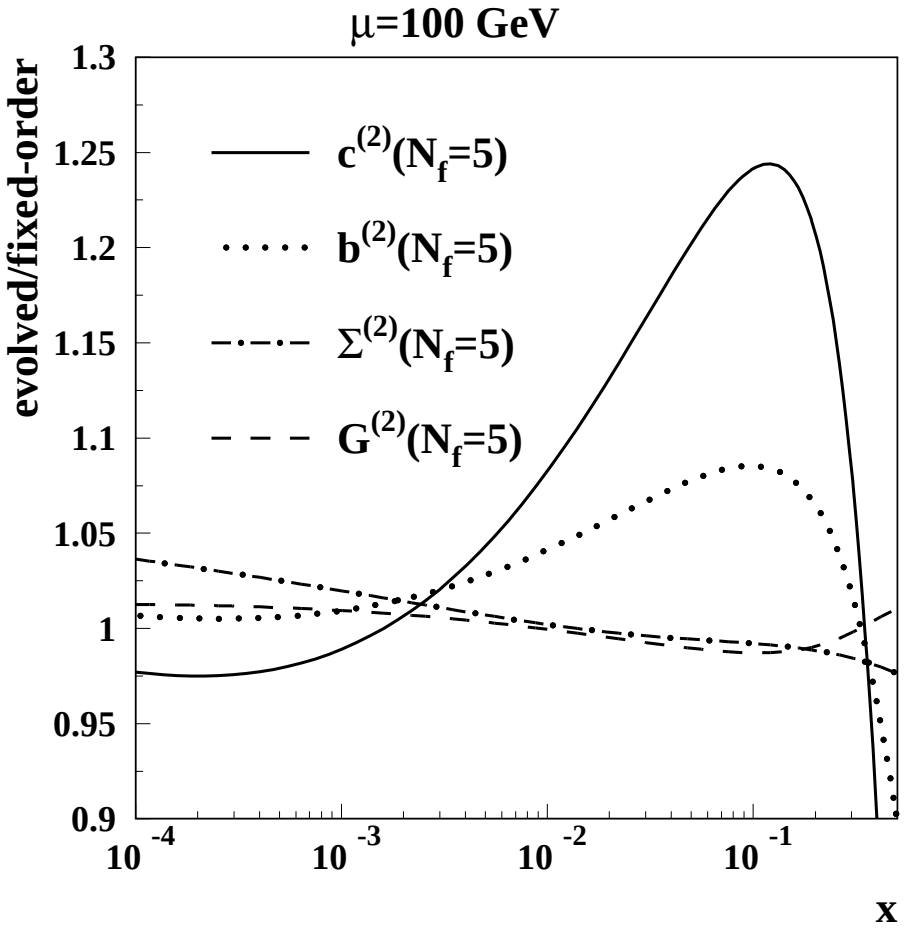

Results for $F_2^c(x, Q^2)$ in GM-VFNS compared to those for FFNS similar to results for PDFs by Alekhin *et al.* in Phys.Rev. D81 (2010) 014032 comparing NNLO evolution to the fixed order result up to $\mathcal{O}(\alpha_S^2)$. Details depend on PDF set and $\alpha_S(M_Z^2)$ value used.

Can lead to over 4% changes in the total $F_2(x, Q^2)$ if the same input PDFs are used in two schemes.

At higher x mainly due to $F_2^c(x, Q^2)$.

At lower x there is a large contribution from light quarks evolving slightly more slowly in FFNS.

At much higher x difference dies away. Charm component becomes very small and light quark evolution not much different. (Light quarks slightly bigger at the highest x.)

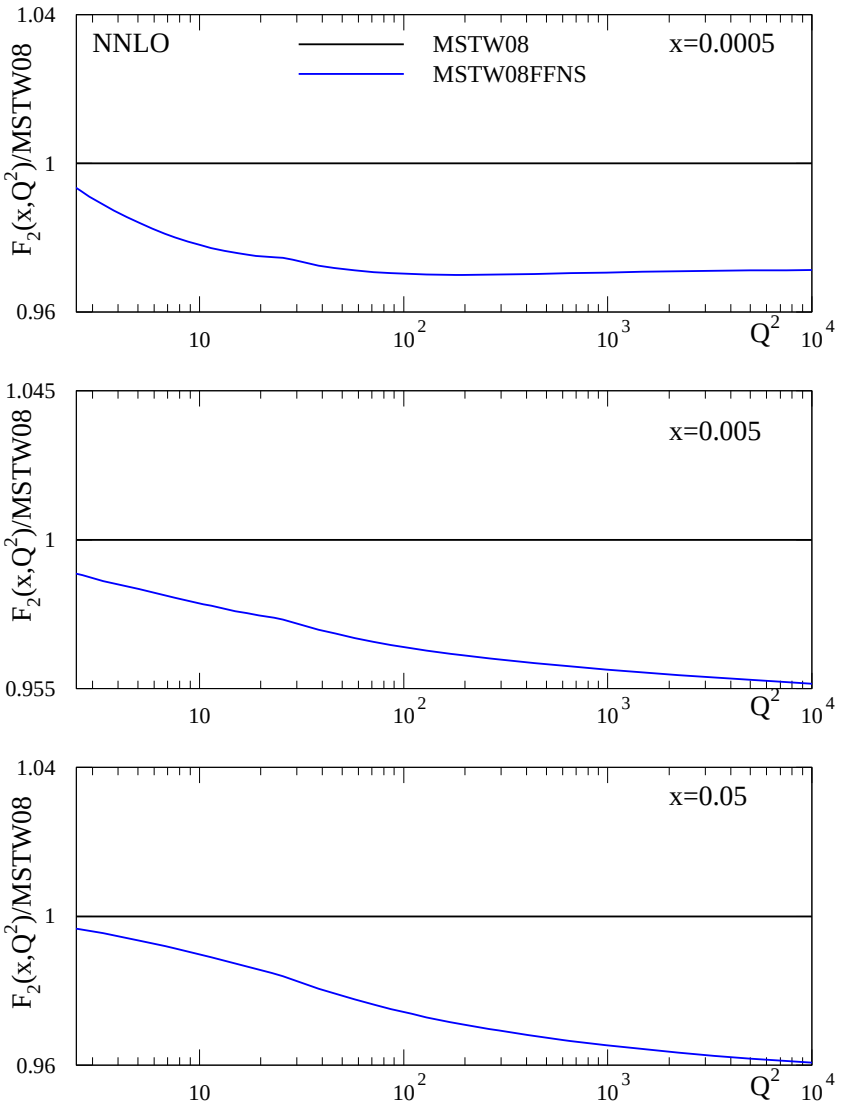

This is certainly important given the precision and range of the data on $F_2(x, Q^2)$ included in PDF fits.

Mainly from HERA, but NMC data also relevant.

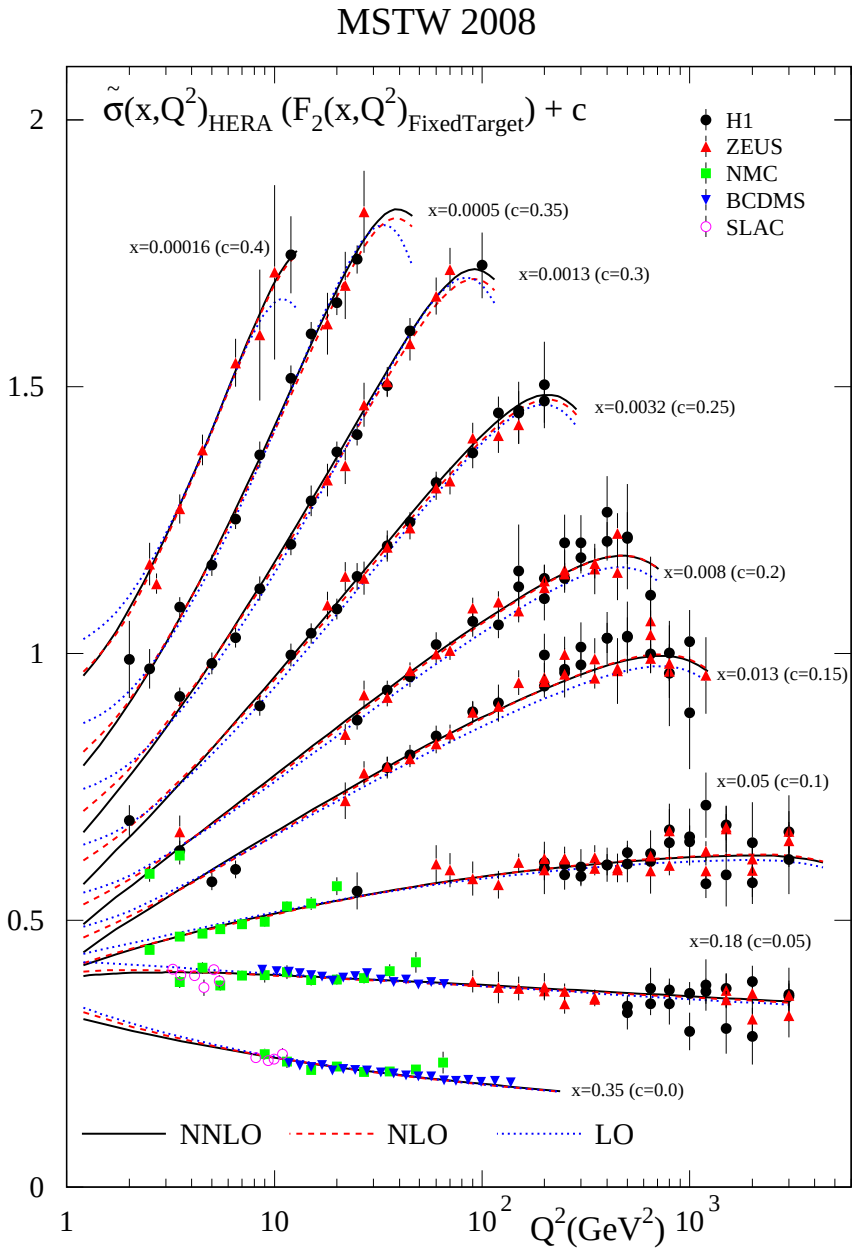

Performed a series of NLO fits using the FFNS scheme and NNLO with up to $\mathcal{O}(\alpha_S^2)$ heavy flavour coefficient functions.(Approximations to the $\mathcal{O}(\alpha_S^3)$ expressions change results very little).

Fit to only DIS and Drell-Yan data but also effectively fit to Tevatron Drell-Yan or Tevatron jet data, if necessary, in 5-flavour scheme as FFNS calculations do not exist.

Fits to DIS and Drell-Yan data usually at least a few tens of units worse than MSTW08 to same data (even without refitting MSTW08 to restricted data sets). Often slightly better for $F_2^c(x, Q^2)$, but flatter in Q^2 for $x \sim 0.01$ for inclusive structure function.

As well as (usually) a worse fit to DIS and Drell-Yan data only, in FFNS the fit quality for the DIS and low-energy Drell Yan data deteriorates by in general ~ 50 units when all jet data is included as opposed to < 10 units when using a GM-VFNS.

PDFs evolved up to $Q^2 = 10,000\mathrm{GeV}^2$ (using variable flavour evolution for consistent comparison) different in form to MSTW08.

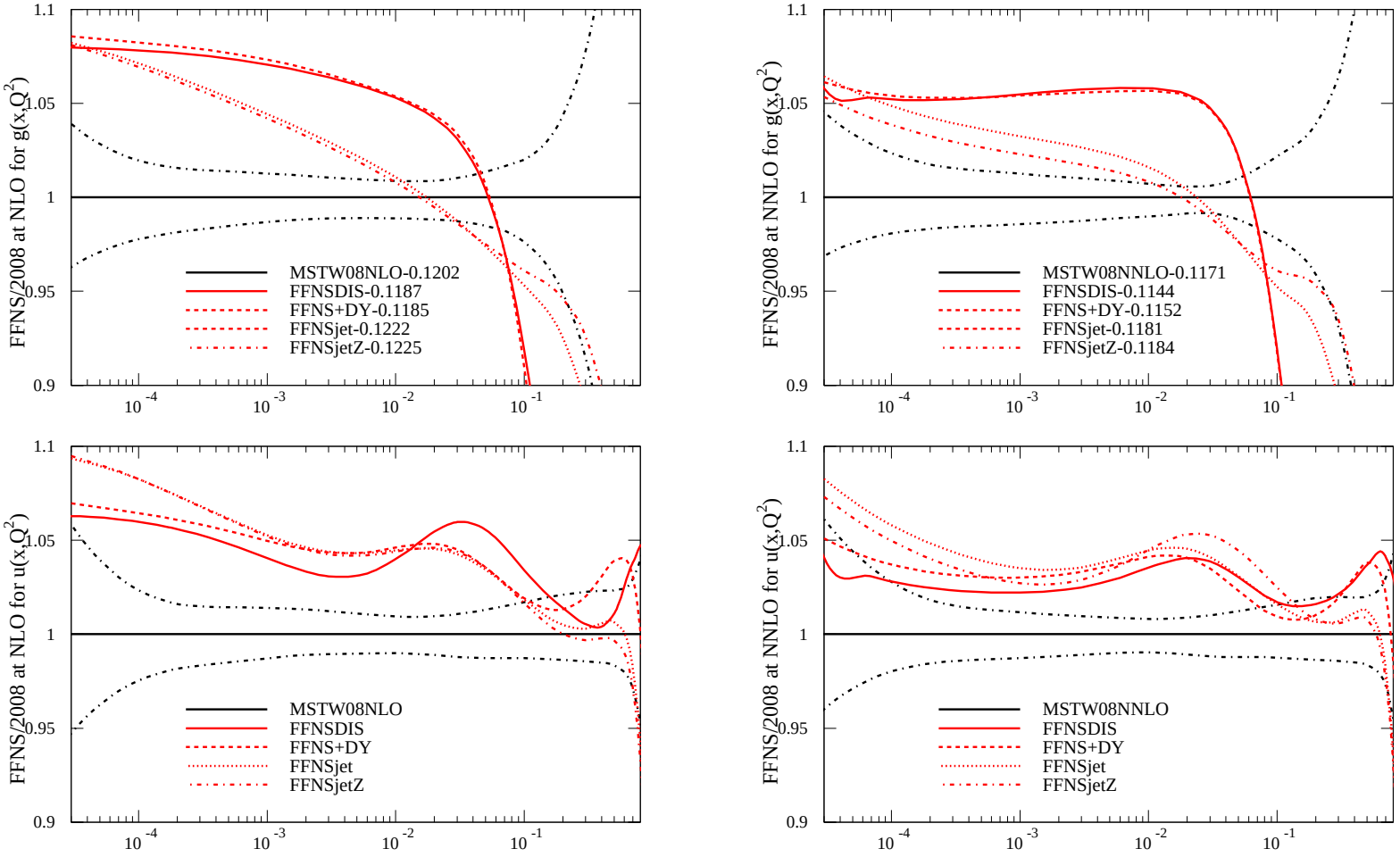

In contrast in standard MSTW2008 fit PDFs usually within uncertainties if Tevatron jet data left out. Main effect loss of tight constraint on $\alpha_S(M_Z^2)$.

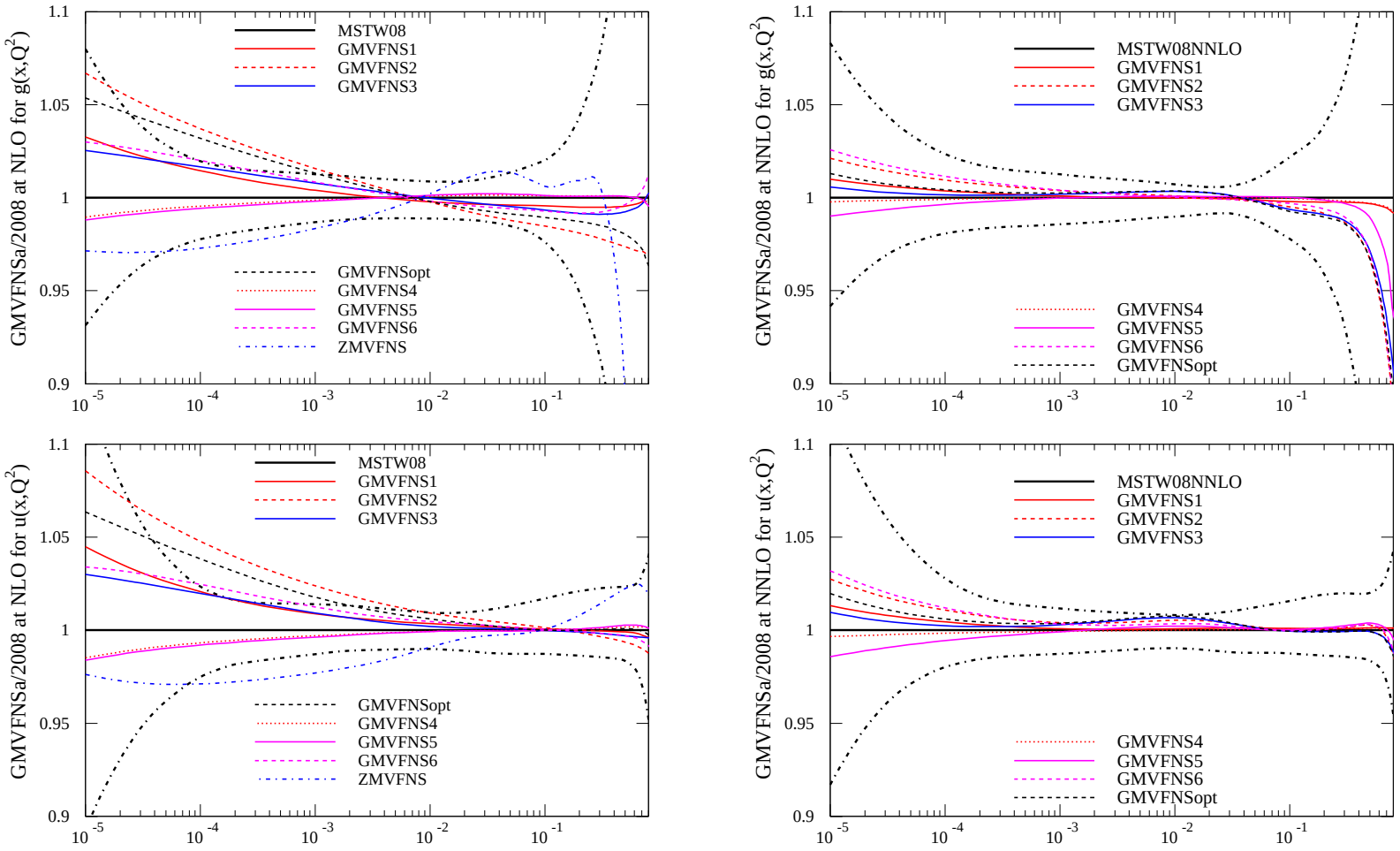

Using FFNS leads to much larger changes than any choice of GM-VFNS mainly due to fitting high-Q^2 DIS data.

Low Q^2 – Higher Twist.

Potentially large corrections at low Q^2 and particularly low W^2. Usual MSTW cuts for

$Q^2_{\rm cut}$ - $2{\rm GeV}^2$

$W^2_{\rm cut}$ - $15{\rm GeV}^2$

Have tried raising Q^2 cut to $5{\rm GeV}^2$ and $10{\rm GeV}^2$ and W^2 to $20{\rm GeV}^2$. Not much effect on PDFs or α_S.

Can also lower $W^2_{\rm cut}$ to $5{\rm GeV}^2$ and try parameterising higher twist contributions by

$$F_i^{\rm HT}(x,Q^2) = F_i^{\rm LT}(x,Q^2)\left(1+\frac{D_i(x)}{Q^2}\right)$$

where i spans bins of x from $x = 0.8 - 0.9$ down to $x = 0 - 0.0005$.

Previously no evidence for much higher twist except at low W^2.

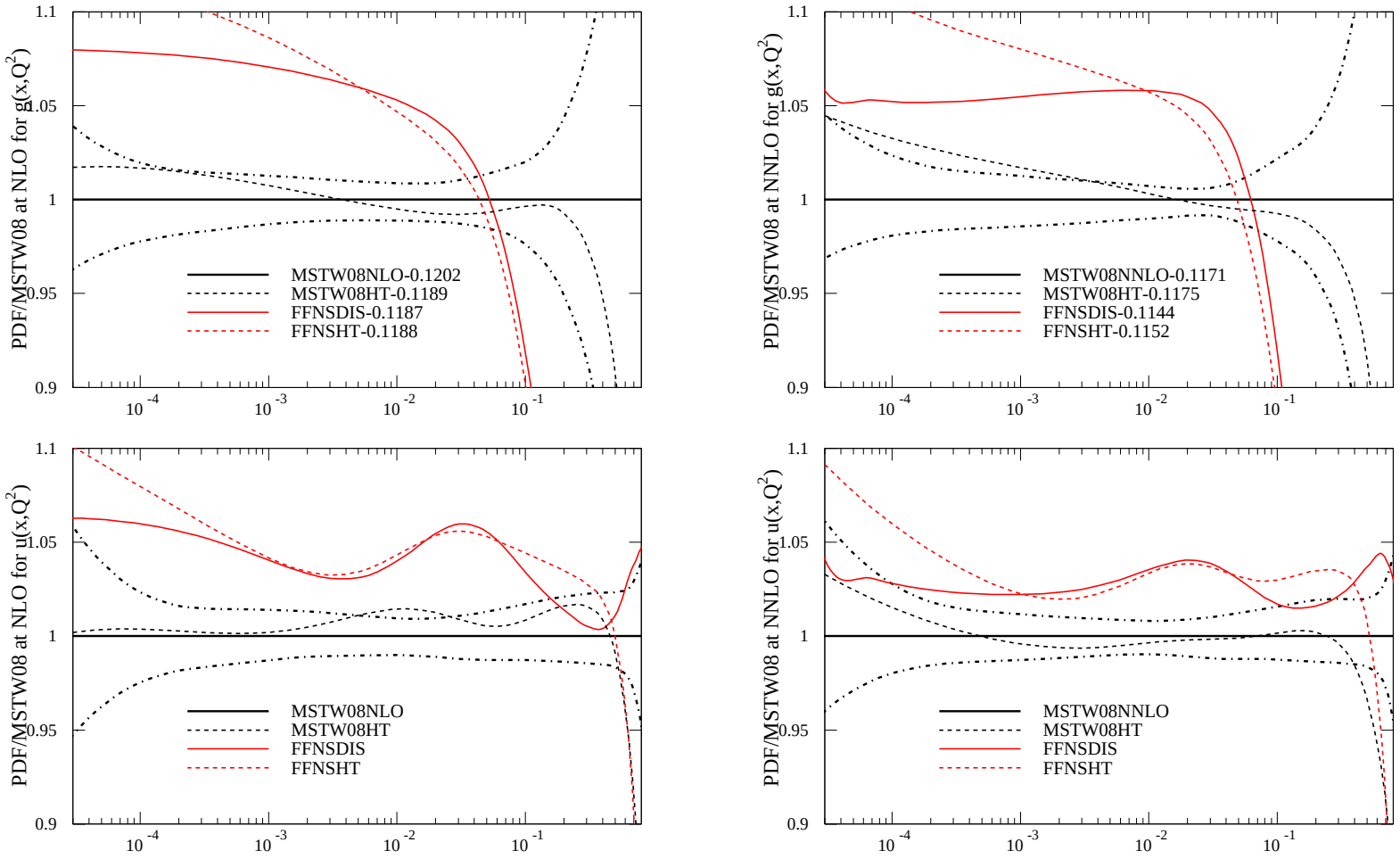

Now more evidence for positive contribution also at very low x. Leads to lower input quarks, more gluon for evolution. Largely washes out quickly with Q^2. Similar effect using FFNS as for GM-VFNS.

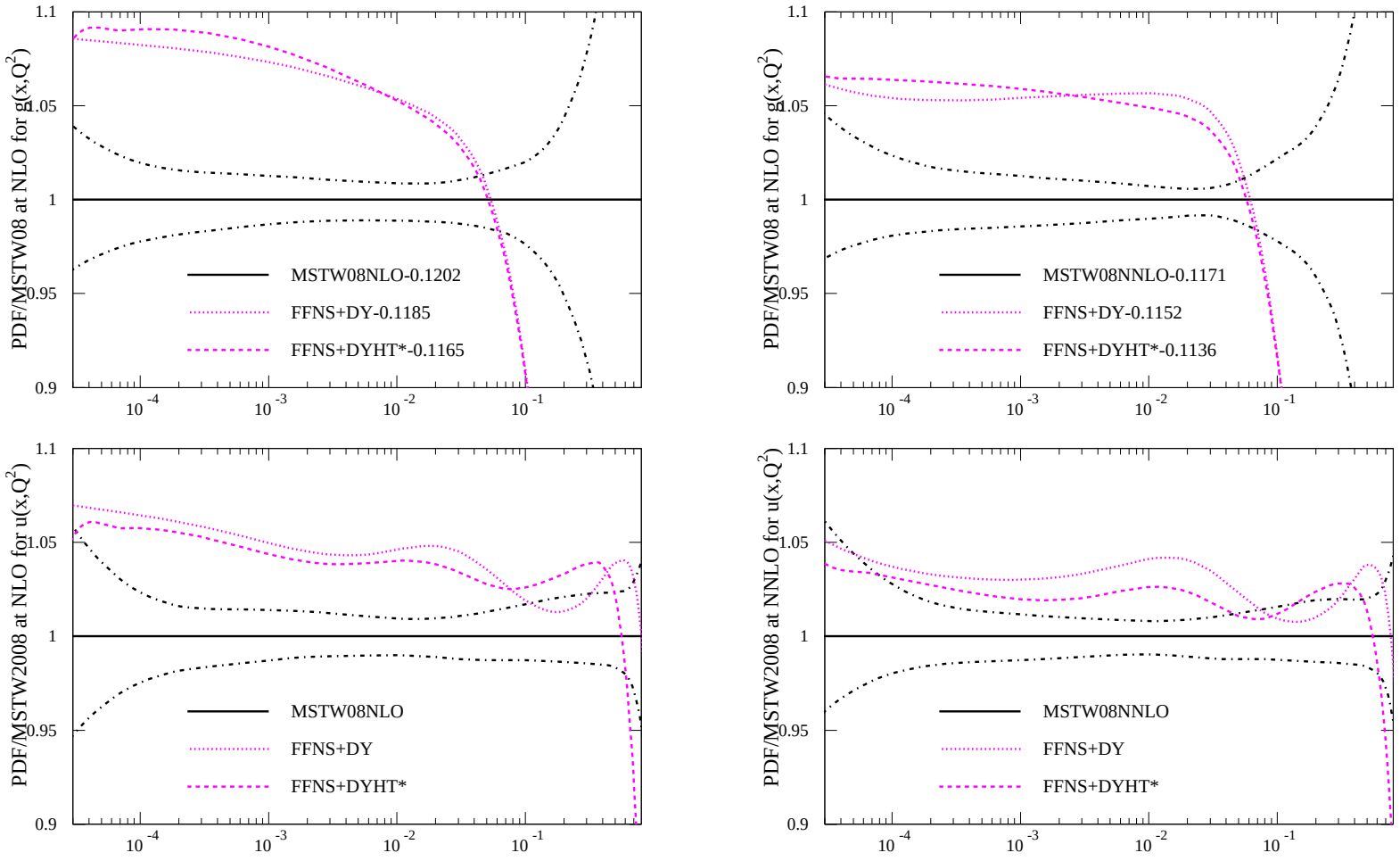

Restricting higher twist from lowest x value and omitting nuclear target data (except dimuon for strangeness) tends to keep values of α_S lower by ~ 0.02.

Explains some PDF differences? MSTW FFNS ratios and ABKM ratios.

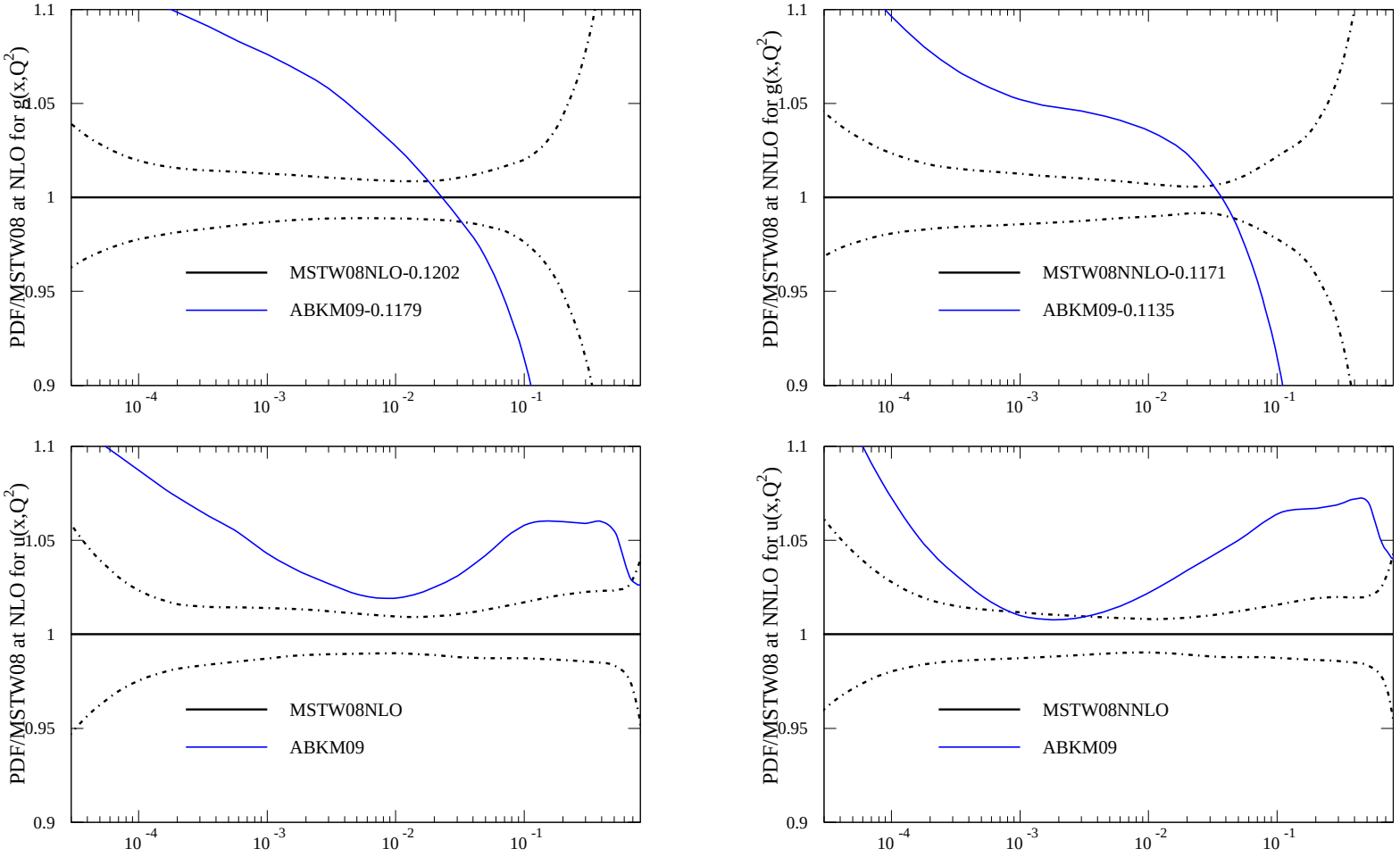

General trend is very similar to fits on previous page.

Conclusions

There is a reasonable amount of variation in comparisons to data/predictions at the LHC using different PDF sets.

The MSTWCP and MSTWCPdeut PDFs improve dramatically the pre(post)diction for lepton asymmetries from W bosons at the LHC.

This is due to a very localised effect in small-x valence quark differences. There is extremely little change in parton luminosities or predictions for a wide variety of other cross sections.

Lowering $W^2_{\rm cut}$ and allowing for higher twist terms in structure functions makes very little change to MSTW PDFs except at extremely high x

Performing fits using an FFNS leads to worse fits to DIS and low energy Drell-Yan data than GM-VFNS, and much more tension with jet data.

Light quarks in variable flavour number scheme are automatically larger in most regions for FFNS than for GM-VFNS. The gluon is smaller at high x and larger at small x in FFNS, and $\alpha_S(M_Z^2)$ smaller. Seems to be the likely explanation of some major differences in PDFs and LHC predictions. (Similar conclusions in NNPDF studies.)

Back-up

Calculate $\chi^2/N = 60/30$ for ATLAS W, Z data again at NLO using APPLGrid. Not best, but fairly close to any other set except CT10 which is best. Again look at eigenvectors.

Fit improves markedly in one direction with eigenvector 9, gluon, which alters common shape and normalisation, and 14 and 18 which alter d_V and u_V, i.e. affect asymmetry. Not much variation in strange normalisation.

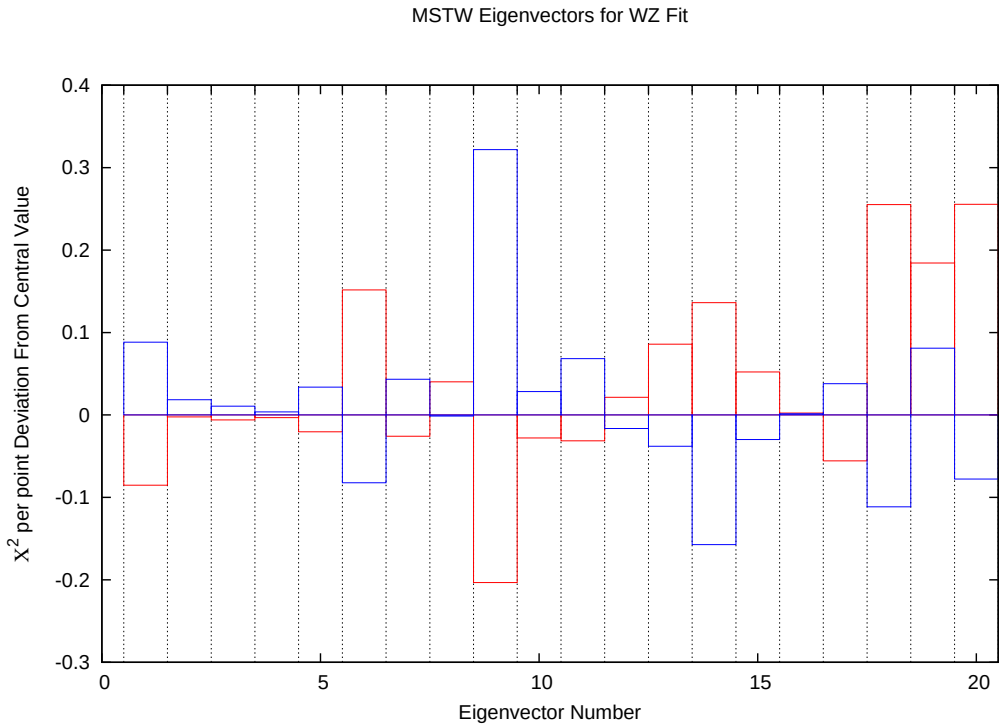

Similar but slightly smaller effect on $u_V - d_V$ than asymmetry alone.

Can also see the effect on the gluon. Slight raise near $x = 0.01$ preferred. Improves overall shape of rapidity distribution. After reweighting $\chi^2 = 48/60$.

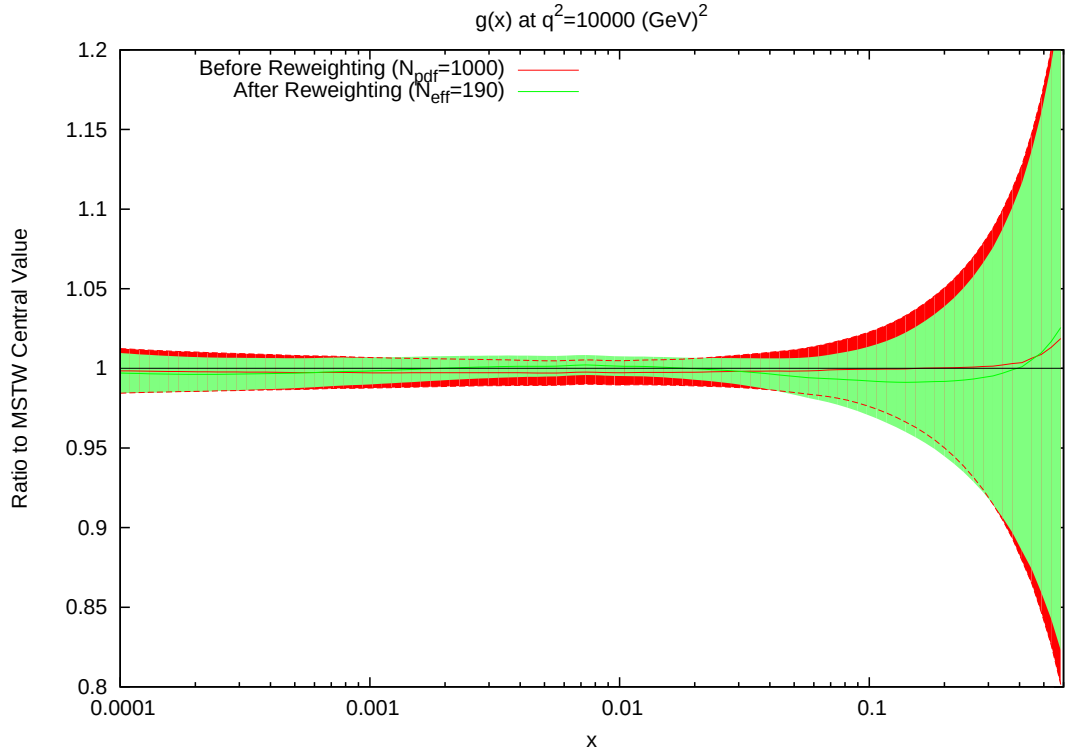

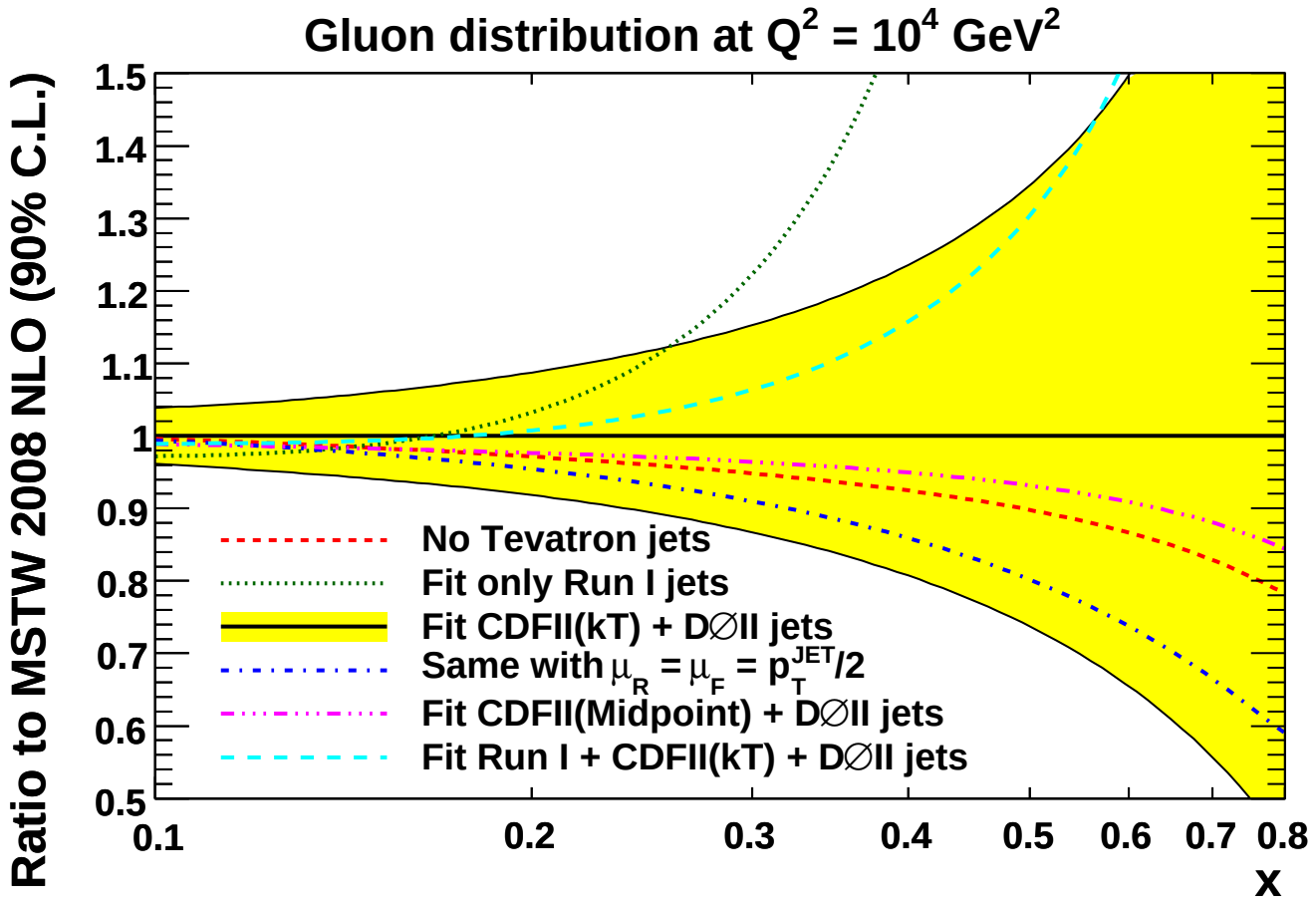

In contrast in MSTW2008 fit central gluon hardly changed if Tevatron jet data left out, and only slight further rearrangement of quark flavours if Drell-Yan data left out.

Main effect loss of tight constraint on $\alpha_S(M_Z^2)$. Much the same at NNLO. Similar results from various other groups.

Given previous relationship between Tevatron asymmetry and deuterium corrections where partial success was noted revisit with extended parameterisation.

Default for MSTW some shadowing for $x < 0.01$.

Previously big improvement in fit, but "unusual" corrections.

Now improvement again but much more stable, and sensible for deuterium corrections. (No shadowing favoured though.)

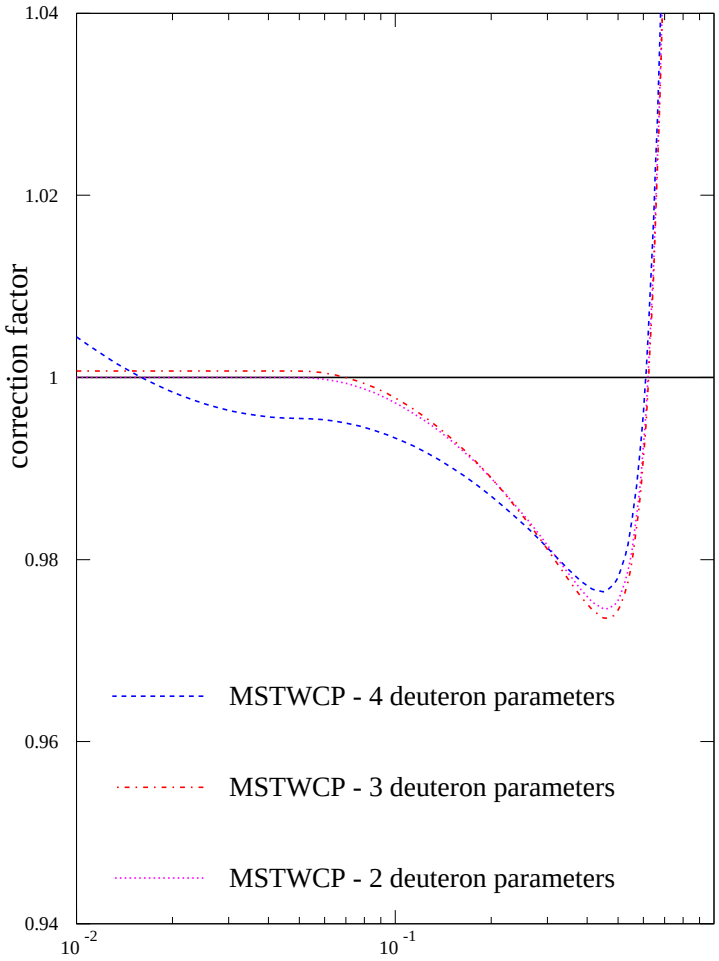

The GM-VFNS can be defined by demanding equivalence of the n_f light flavour and n_f+1 light flavour descriptions at all orders – above transition point $n_f \to n_f+1$

$$F(x,Q^2) = C_k^{FF,n_f}(Q^2/m_H^2) \otimes f_k^{n_f}(Q^2) = C_j^{VF,n_f+1}(Q^2/m_H^2) \otimes f_j^{n_f+1}(Q^2)$$
$$\equiv C_j^{VF,n_f+1}(Q^2/m_H^2) \otimes A_{jk}(Q^2/m_H^2) \otimes f_k^{n_f}(Q^2).$$

Hence, the VFNS coefficient functions satisfy

$$C_k^{FF,n_f}(Q^2/m_H^2) = C_j^{VF,n_f+1}(Q^2/m_H^2) \otimes A_{jk}(Q^2/m_H^2),$$

which at $\mathcal{O}(\alpha_S)$ gives

$$C_{2,Hg}^{FF,n_f,(1)}(\frac{Q^2}{m_H^2}) = C_{2,HH}^{VF,n_f+1,(0)}(\frac{Q^2}{m_H^2}) \otimes P_{qg}^0 \ln(Q^2/m_H^2) + C_{2,Hg}^{VF,n_f+1,(1)}(\frac{Q^2}{m_H^2}),$$

The VFNS coefficient functions tend to the $m=0$ limits as $Q^2/m_H^2 \to \infty$.

However, $C_j^{VF}(Q^2/m_H^2)$ only uniquely defined in this limit.

Can swap $\mathcal{O}(m_H^2/Q^2)$ terms between $C_{2,HH}^{VF,0}(Q^2/m_H^2)$ and $C_{2,g}^{VF,1}(Q^2/m_H^2)$.

The results for $F_2(x, Q^2)$ when refits are performed.

As seen very little change when using GM-VFNS with no jets.

Much more tension and worse fits for FFNS.

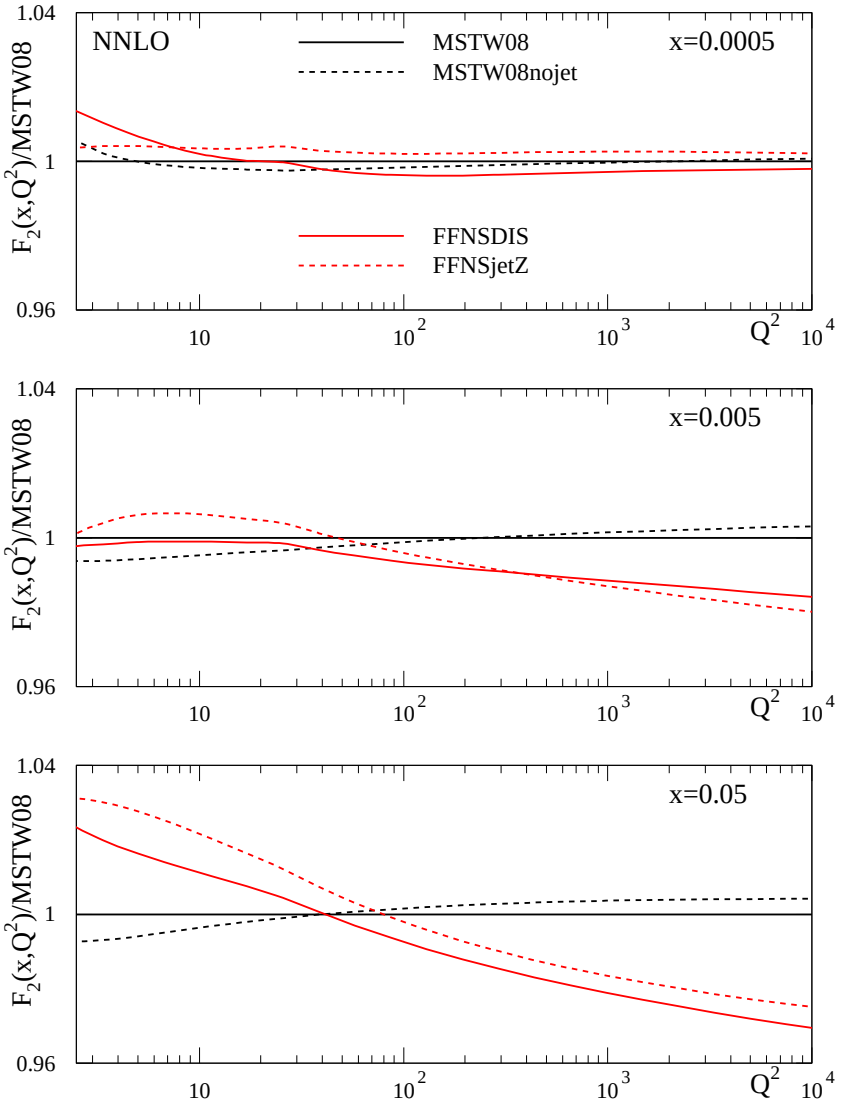

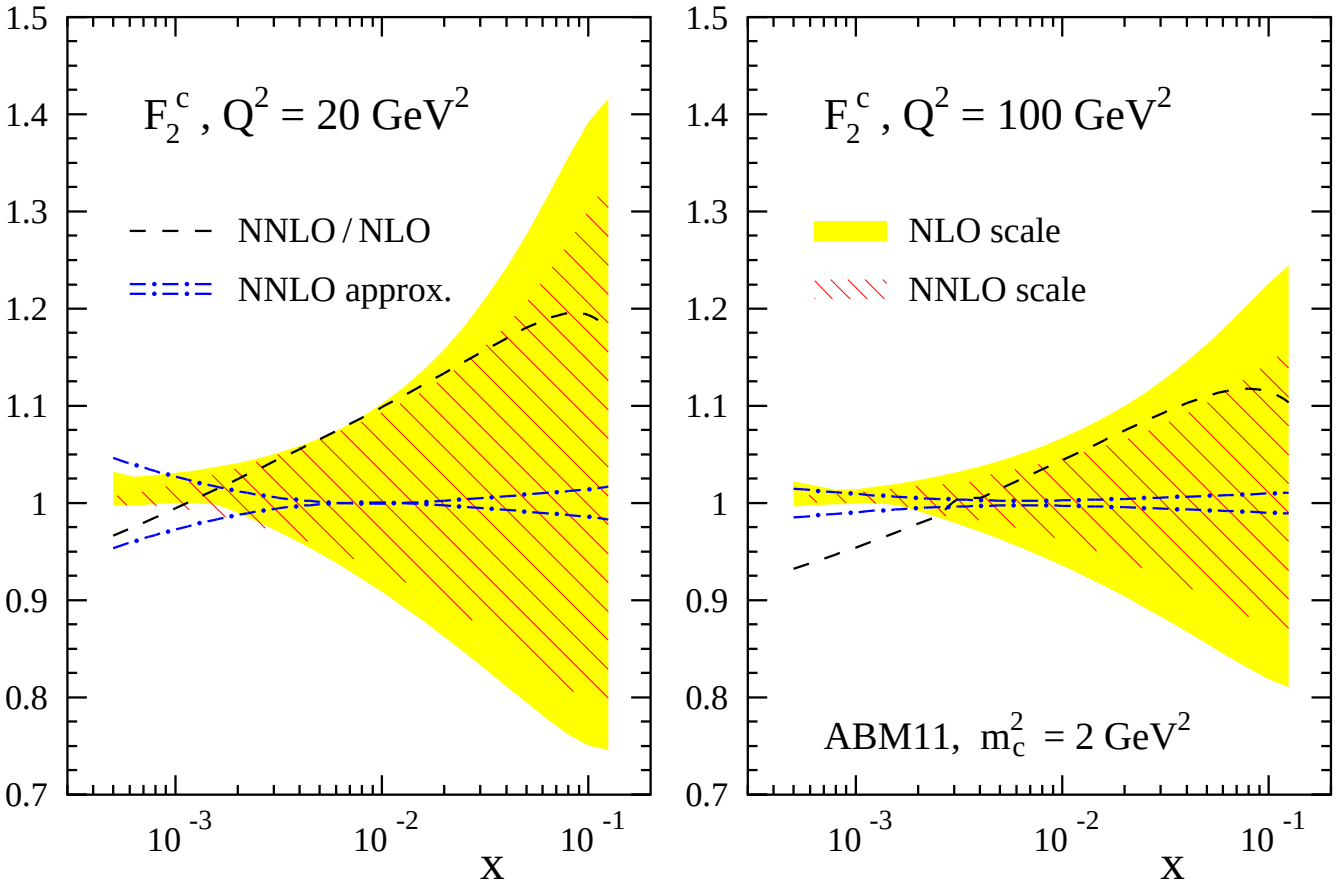

Approximate $\mathcal{O}(\alpha_S^3)$ corrections to $F_2^c(x, Q^2)$ by Kawamura *et al.* in Nucl.Phys. B864 (2012) 399-468.

Similar results for $\mathcal{O}(\alpha_S^3)$ approximation used by MSTW at low Q^2 extended to higher Q^2.

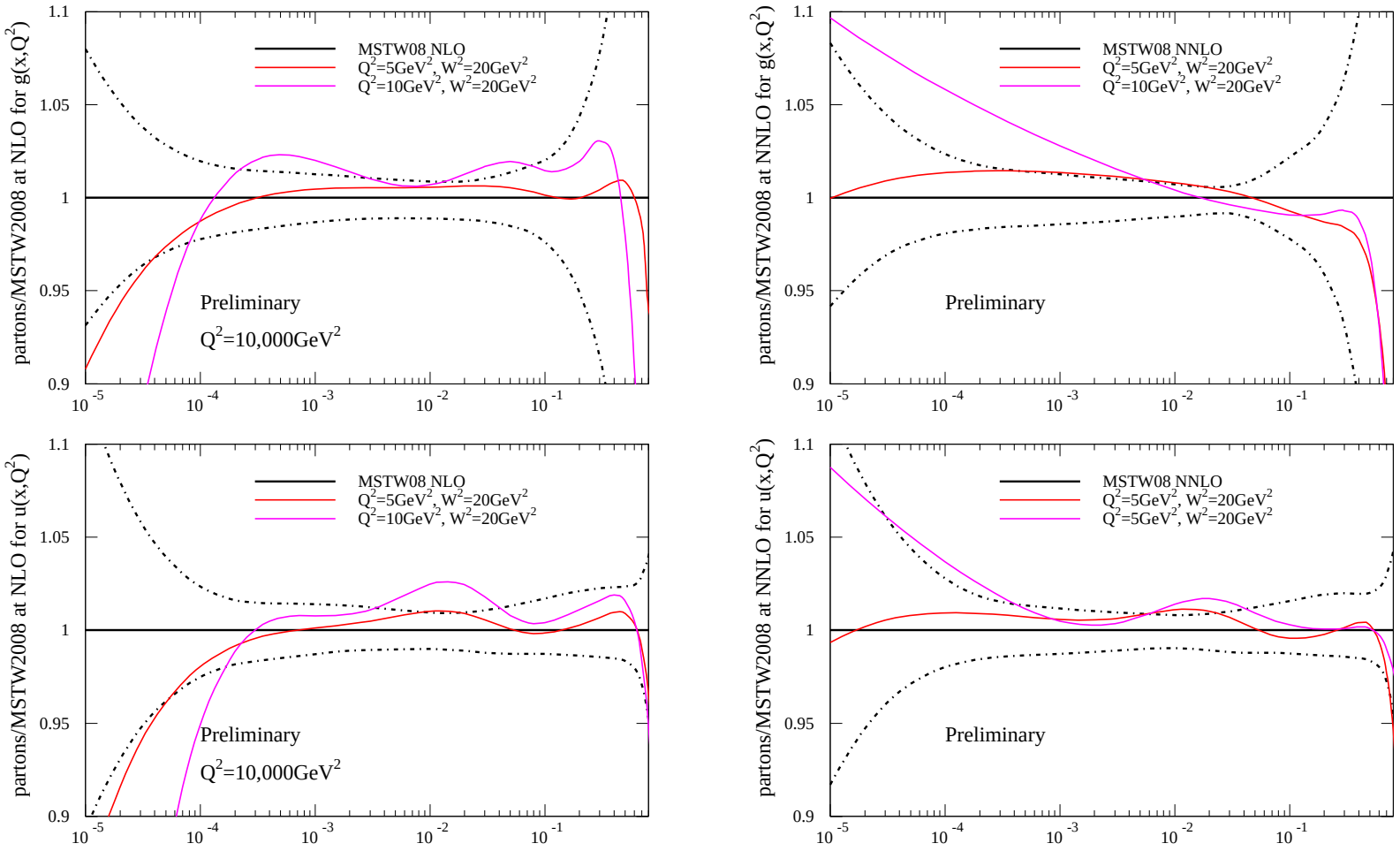

Similar to effect of higher twist, particularly at NNLO. Remember lose data at lowest x.

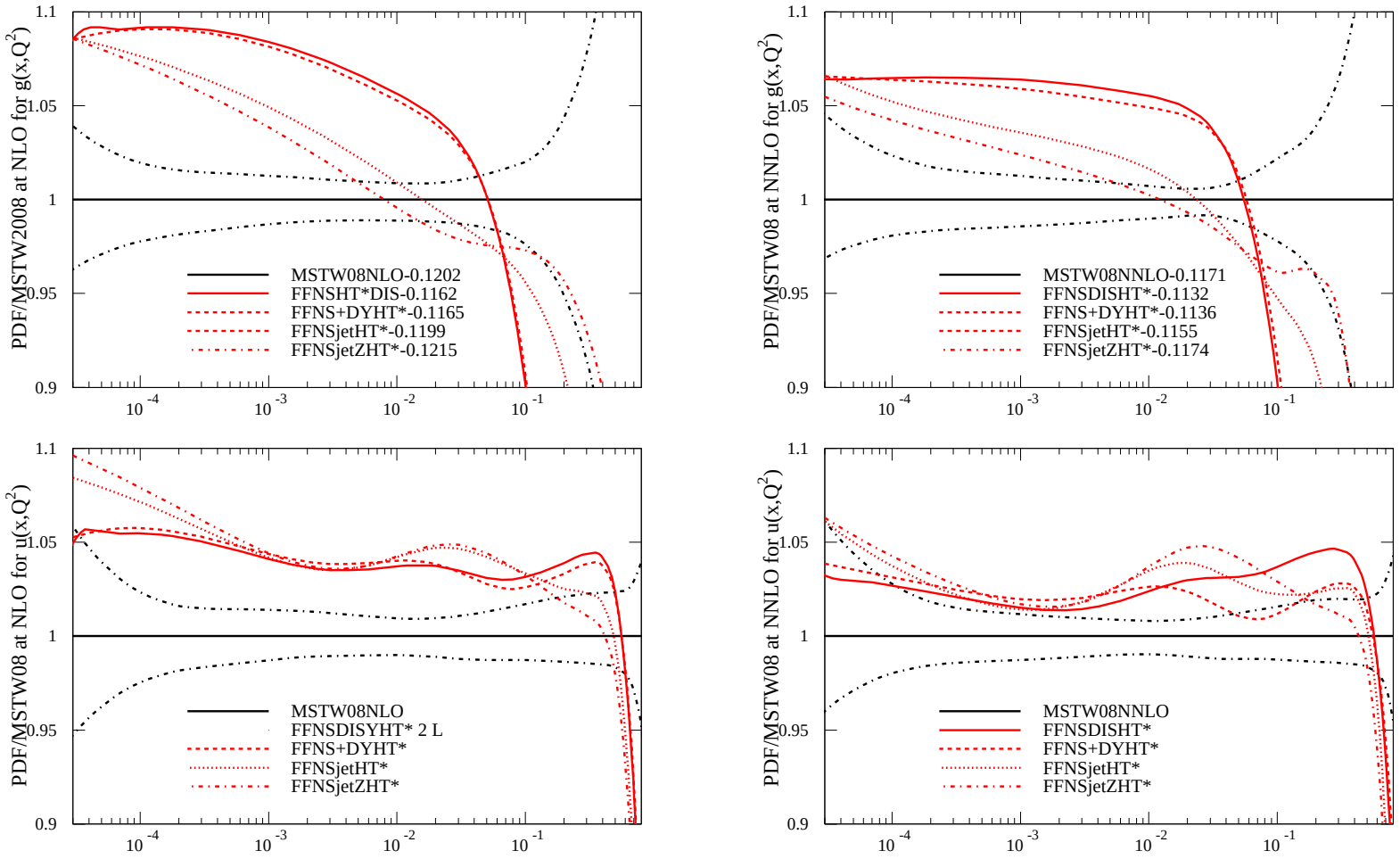

Restricting higher twist from lowest x value and omitting nuclear target data (except dimuon for strangeness). Same trends as for standard fits but slightly lower α_S

Explains some PDF differences? MSTW FFNS ratios and ABKM ratios.

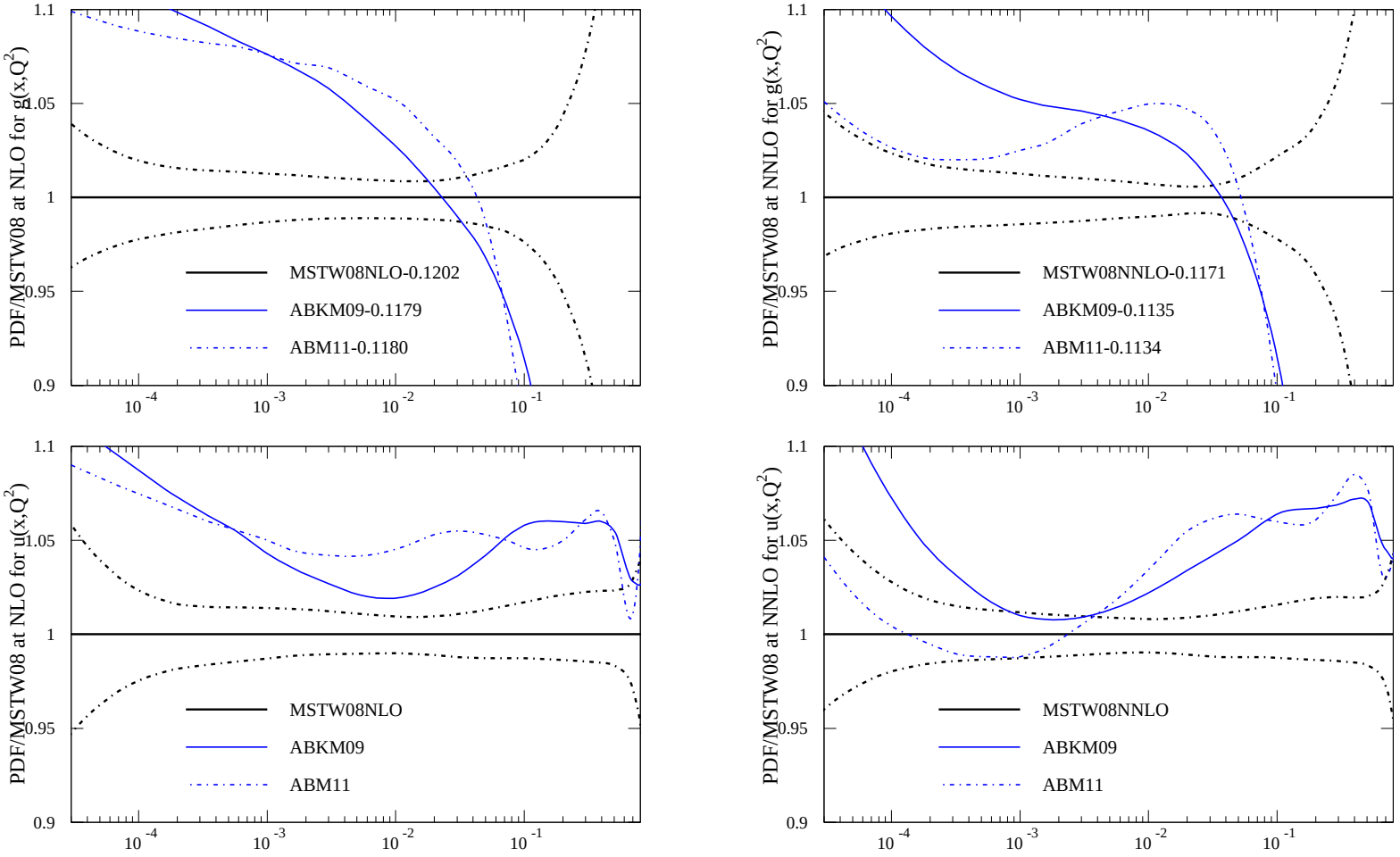

Better to compare to ABKM09 as mass scheme and data fit are more similar.

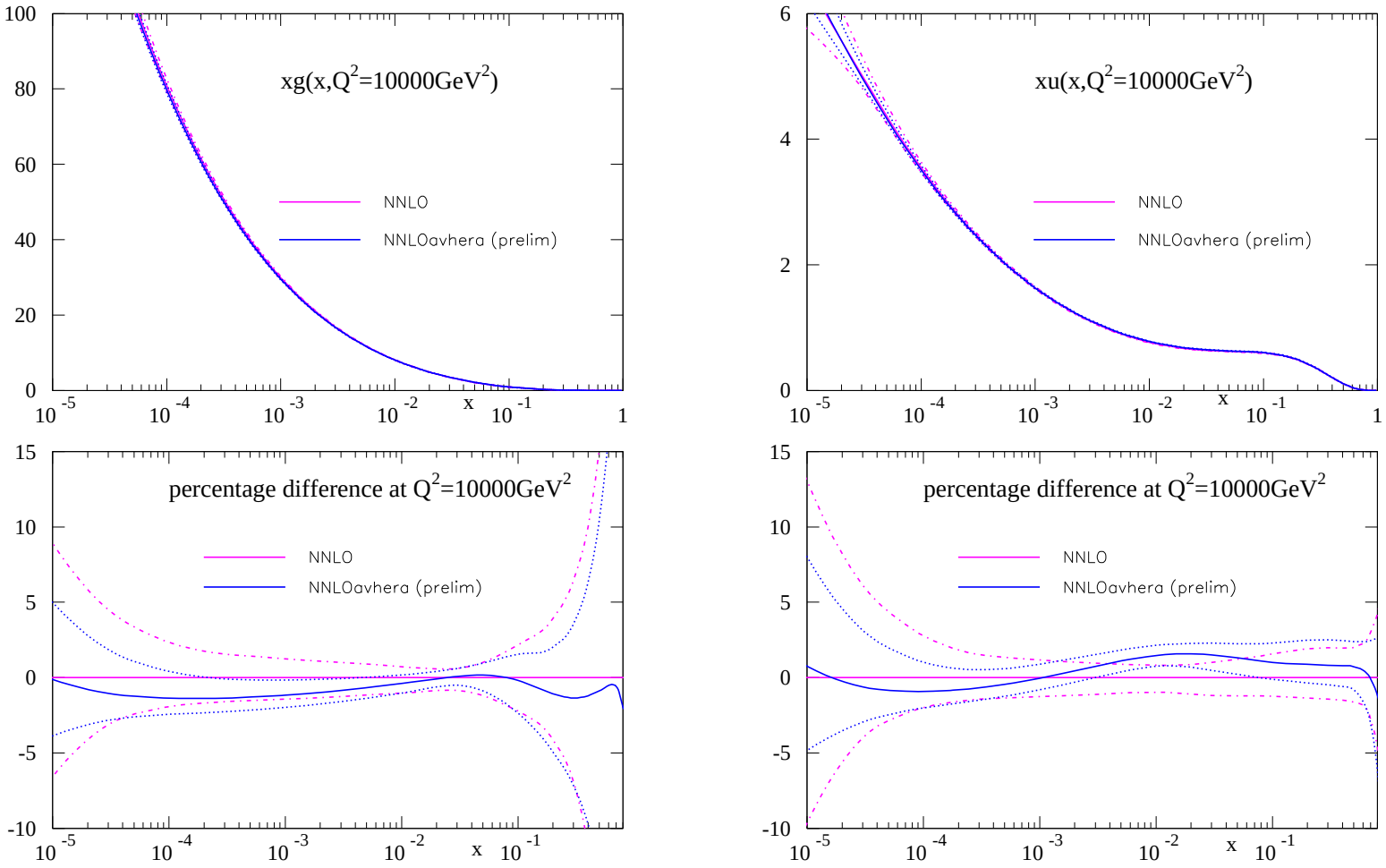

Change in MSTW2008 NNLO PDFs when fitting HERA combined data.

Comparison to LHC data.

Start with ATLAS jets. Use APPLGrid or FastNLO at NLO (Ben Watt) and correlated errors treated as in the formula,

$$\chi^2 = \sum_{i=1}^{N_{\rm pts.}} \left(\frac{\hat{D}_i - T_i}{\sigma_i^{\rm uncorr.}} \right)^2 + \sum_{k=1}^{N_{\rm corr.}} r_k^2,$$

where $\hat{D}_i \equiv D_i - \sum_{k=1}^{N_{\rm corr.}} r_k \, \sigma_{k,i}^{\rm corr.} D_i$ are the data points allowed to shift by the systematic errors in order to give the best fit, and $\sigma_{k,i}^{\rm corr.}$ is a fractional uncertainty. Normalisation is treated as the other correlated uncertainties.

MSTW fit very good (χ^2 per point below left), though numbers lower for inclusive data. Always close to, if not best, particularly for $R = 0.6$. Not huge variation in PDFs though.

Scale	pT/2	pT	2pT
Inclusive (R=0.4)	0.752	0.773	0.703
Inclusive (R=0.6)	0.845	0.790	0.721
Dijet (R=0.4)	2.53	2.24	2.20
Dijet (R=0.6)	2.44	2.04	1.74

	$\lvert r_k\rvert < 1$	$1 < \lvert r_k\rvert < 2$	$2 < \lvert r_k\rvert < 3$	$3 < \lvert r_k\rvert < 4$
Inclusive (R=0.4)	85	2	1	0
Inclusive (R=0.6)	87	1	0	0
Dijet (R=0.4)	82	6	0	0
Dijet (R=0.6)	74	12	2	0